Phosphatase activity of soluble Epoxide Hydrolase (sEH)

Thesis Submitted to School of Science and Technology,
Kwansei Gakuin University,
for the Doctor of Science Degree

By
Endang Rinawati Purba
2014

[CONTENTS]

Page

Abstract

Soluble epoxide hydrolase (sEH) is an enzyme with multiple functions that has two distinct enzyme activities: epoxide hydrolase (C-terminal domain) and phosphatase (N-terminal domain). The endogenous substrates of epoxide hydrolase are epoxyeicosatrienoic acids (EETs) that are hydrolyzed by sEH to corresponding diols, dihydroxyeicosatrienoic acids (DHETs). The N-terminal domain metabolizes lysophosphatidic acids (LPAs). In this study, I investigated the catalytic activity of sEH isolated from *Xenopus laevis* and the metabolism of lysophosphatidic acids (LPAs) by allelic variants of human sEH. Firstly the catalytic activities of both N/C terminal domains of sEH were investigated. *Xenopus* sEH cDNA was isolated from embryos of *Xenopus laevis*. The *Xenopus* sEH was expressed in *Escherichia coli* and was purified. The purified *Xenopus* sEH did not show phosphatase activity toward 4-methylumbelliferyl phosphate (4-MUP) or several LPAs although it had EH activity. The epoxide hydrolase activity of sEH seemed to be similar to that of human sEH, while *Xenopus* sEH did not have phosphatase activity toward several substrates that human sEH metabolizes. In contrast, to elucidate the sEH phosphatase activity that metabolizes LPAs, the human sEH were used. A purified wild-type (WT) and six allelic variants of sEH (K55R, R103C, C154Y, R287Q, V422A, and E470G) were used in this study. The R103C and R287Q variants revealed significant lower activity than WT sEH. The kinetic study indicated that R103C and R287Q variants had lower *V*max/*K*m ratio toward stearoyl-LPA than other variants. Regarding the effect of sEH allelic variants on VEGF expression, all variants except V442A revealed suppressed VEGF mRNA levels in Hep3B cells. These results suggest that the R103C and R287Q variants have lower phosphatase activity, however, all allelic variants except V442A have similar effect to the VEGF suppression.

General Introduction

sEH enzymes are widely present in all living organisms, such as mammal, bacteria, yeast, and fungi. The sEH enzyme plays a significant role in the detoxification, catabolism, and regulation of signaling molecules. sEH has two domains: N-terminal phosphatase domain and C-terminal epoxide hydrolase domain. The C-terminal domain is connected via a proline-rich linker to a smaller N-terminal domain. The C-terminal epoxide hydrolase catalytic activity has been well studied. The epoxide hydrolase (EH) are enzymes that catalyze the hydrolysis of exogenous and endogenous epoxide to their corresponding diols by addition of water. The C-terminal epoxide hydrolase sequences are member of the α/β hydrolase fold superfamily. In the C-terminal domain, D335, D496, and H524 are catalytic active sites that are together called the catalytic triad for epoxide hydrolase activity [1]. In contrast, a function of N-terminal phosphatase that has high homology to the haloacid dehalogenase family of phosphatases, remain less studied. In this study, characterization of sEH catalytic activity of *Xenopus laevis* was investigated. On the other hand, the mutated residues of human sEH allelic variants were examined to understand the effect of these variants on the metabolism of lysophosphatidic acids (LPAs). These investigations may useful for further clarifying the role of sEH phosphatases functions.

The endogenous substrate of EH is epoxyeicosatrienoic acids (EETs). EETs are generated by the activity of both selective and also more general cytochrome p450 (CYP) enzymes on arachidonic acid and inactivated largely by sEH, which converts them to their corresponding dihydroxyeicosatrienoic acids (DHETs). The biological effects of EETs are terminated through its metabolism by sEH to DHETs. sEH is largely critical in the control of EET levels because of its ability to catalyze the degradation of EETs into diols [2]. In mice and Zebrafish, inactivation of sEH decreased progenitor cell proliferation [3]. On the other hand, in previous study LPAs found to be the endogenous

substrates for the phosphatase activity [4]. Isoprenoid phosphatase was also found to be a phosphatase substrate of sEH [5]. Several lines of evidence indicate a biological role for sEH phosphatase activity (N-terminal domain). In mice, it seems that the N-terminal domain play a role in the development of hypoxia-induced pulmonary hypertension [6]. In this study, the characterization of important phosphatase activity in *Xenopus* sEH was evaluated by the comparison with human sEH.

In comparison with mammal sEH, little is known about sEH of *Xenopus laevis*. *Xenopus* sEH displays high homology to the C-terminal domain of the human sEH that contains the amino acid residue critical to catalytic activity. However, several residues of catalytic active site on the N-terminus of human sEH is not conserved in *Xenopus* sEH. The previous investigation in animal models showed sEH catalytic activity in the sea urchin (*Strongylocentrotus purpuratus*) [7], *Caenorhabditis elegans* [8], and chicken (*Gallus gallus*) [7]. However, the EH and phosphatase activities in frog sEH were not investigated. In Chapter I, the isolation and characterization of *Xenopus* sEH will provide information on the role of sEH enzymatic activity. For our knowledge, this is the first study to characterize *Xenopus* sEH.

In mammalian sEH, single nucleotide polymorphisms (SNPs) of sEH were found and several allelic variants displays different epoxide hydrolase activity [9,10]. Most of the biological roles of sEH allelic variants have been attributed to its more well defined on EH activity. Endogenous EH substrates include arachidonic acid and linoleic acid epoxide, which have been shown to regulated blood pressure [11] and inflammation [12]. The R103C amino acid substitution was associated with increased cell death induced in cortical neuron by oxygen-glucose deprivation and re-oxygenation [13]. The R287Q variant is associated with increased plasma cholesterol levels in familial hypercholesterolemia [14], the onset on coronary artery calcification in Africa-American individuals [15], and insulin resistance in type 2 diabetic [16]. However,

the effect of allelic variants of human sEH on the phosphatase activities toward other LPAs remains unknown. In Chapter II, the catalytic activities of human sEH allelic variants were examined to understand the effect of these variants on the metabolism of LPAs.

LPA is a bioactive phospholipid with diverse physiological action on many of cells types. LPA signaling are large views on the potential pathway in human diseases that include cardiovascular and cancer [17,18]. Previously we found the LPAs are endogenous substrate of sEH. In addition, phosphatase domain contributed to the expression of vascular endothelial growth factor (VEGF) and cell growth [19]. The variants R103 and R287 of sEH are promising research area in the direction of signaling molecule associated with the human diseases such as cardiovascular and cancer. In the present experiment, six allelic variants of sEH were expressed in the Hep3B cells to understand the effect of these variants on VEGF suppression. The major disease areas associated with LPA as described above and sEH allelic variant may reveal a linkage between LPA and phosphatase activity. In Chapter II, the action of sEH on several LPAs could explain the biological functions associated with the phosphatase activity. The metabolism of LPA, phosphatases, and sEH allelic variant might contribute to provide new insight on the role of this matter in the near future.

CHAPTER I

Isolation and characterization of *Xenopus* soluble epoxide hydrolase

I.1 Introduction

Soluble epoxide hydrolase (sEH) is a ubiquitous enzyme in vertebrates that transform epoxides to their corresponding diols [20,21]. Human sEH has 555 amino acid residues containing N-terminal and C-terminal domains. The N-terminal domain has 1-209 amino acid residues and the C-terminal domain has 217-555 amino acid residues. The C-terminal domain is connected via a proline-rich linker to a smaller N-terminal domain. sEH has two distinct enzyme activities: N-terminal phosphatase activity and C-terminal epoxide hydrolase activity [6,22]. In the N-terminal domain, a substitution of D11, T123, N124 or D185 leads to sEH mutant protein having altered kinetic properties. In contrast, substitution of D9, K160, D184 or N189 resulted in a complete loss of phosphatase activity consistent with an essential function for catalytic activity [23]. In the C-terminal domain, D335, D496, and H524 are catalytic active sites that are together called the catalytic triad for epoxide hydrolase activity [1]. The catalytic activity of human sEH has been found and explained by the action of the C-terminal domain alone. Therefore, the recombinant human sEH lacking the C-terminal domain also displays phosphatase activity [6,24]. Mammalian soluble epoxide hydrolase consisting of EH and phosphatase domain is though to be a product of the fusion of two ancestral bacteria: haloalkane dehalogenase and haloacid dehalogenase. The N-terminal domain of sea urchin (*Strongylocentrotus purpuratus*) lacks residues thought to be important for sEH phosphatase activity [7]. No predicted enzymes correspond to full-length sEH in the genome of *Caenorhabditis elegans* [8]. Chicken (*Gallus gallus*) sEH has high homology of the N-terminal domain with the human sEH but lack phosphatase activity [7]. However, EH and phosphatase activities in amphibian sEH were not investigated. In this study, the characterization of *Xenopus* sEH will provide information on the role of sEH enzymatic activity.

sEH is a key enzyme in the metabolic conversion or degradation of epoxyeicosatrienoic acids [25] which are produced by cytochrome P450 (CYP) epoxygenase from arachidonic acid [25,26]. The biological effects of EETs are terminated through its metabolism by sEH to dihydroxyeicosatrienoic acids (DHETs), a process that serves as a key regulator of tissue EET levels [27]. In mice, sEH inactivation attenuated progenitor cell proliferation but the sEH products 12, 13-dihydroxyoctadacenoic acid (12, 13-DiHOME) and 11, 12-dihydroxyeicosatrienoic acid stimulated canonical Wnt signaling and rescued the effect of sEH inhibition. In Zebrafish, sEH downregulation/inhibition impaired the development of the caudal vein plexus and decreased the number of progenitor cells [3].

Previously it was found that lysophosphatidic acids (LPAs) are substrates for the phosphatase activity of human sEH [4]. Isoprenoid phosphatase was also found to be a substrate of sEH [5]. Several lines of evidence indicate a biological role for sEH phosphatase activity (N-terminal domain). The sEH-null mice that lack both epoxide hydrolase and phosphatase activities have lower cholesterol and steroid levels [28]. In mice, it seems that the N-terminal domain play a role in the development of hypoxia-induced pulmonary hypertension [6]. Furthermore, our previous study found the phosphatase domain contributed to the expression of vascular endothelial growth factor (VEGF) and cell growth [19].

The aim of this study is to clarify the characterization of *Xenopus* sEH catalytic activity. To our knowledge, this is the first study to characterize *Xenopus* sEH.

I.2 Materials and methods

Eggs and embryos of *Xenopus laevis*

Eggs were obtained from female *Xenopus laevis* (Watanabe Zoushoku, Hyogo, Japan) by human chorionic gonadotropin injection. Eggs were raised in chestnuts suspended in 1.0 x Modified Birth's Solution (MBS), 0.5 mM HEPES, pH 7.5, containing 10 mM NaCl, 0.2 mM KCl, 0.1 mM $MgCl_2$, 0.2 mM $CaCl_2$. The chestnuts were isolated from a male by surgical operation. The fertilized embryos were dejellied using 2% cysteine and washed with 0.1 x MBS several times. Embryos were staged according to Nieuwkoop and Feber's normal table [29]. The embryos were cultured in 60 mm glass dishes containing 15 mL medium at 18^0C.

Isolation of RNA and Reverse transcription-PCR

Total RNA was extracted from eggs at various stages (0, 10.5, 18, 23, 26, 30 and 38) and converted to cDNA using reverse transcriptase (Fermentas, Burlington, Ontario, Canada) according to the manufacturer's instructions as follows: incubation at 25^0C for 15 min and at 42^0C for 60 min, followed by heating at 70^0C for 10 min. The DNA sequences of the primers used in this study are shown in Table I-1. PCR was performed with primers 1 and 2 for *Xenopus* sEH and with primers 3 and 4 for *histone-H4* under the following conditions: denaturation at 94^0C for 2 min and 27 and 23 cycles, respectively, 94^0C for 30 sec, 55^0C for 30 sec, and 72^0C for 30 sec. The reaction mixtures contained 10 pmol specific primers and Go Taq Green Master Mix was acquired from Promega (Madison, WI). DNA fragments were separated on an agarose gel and visualized with ethidium bromide staining. Bands of gel images were quantified by Scion Image software version 4.03 (National Institutes of Health, Bethesda, MD).

Detection of *Xenopus sEH* mRNA in various tissues and embryos

Expression of *Xenopus sEH* mRNA was detected by RT-PCR at various *Xenopus* embryo stages and in several tissues. Tissues were collected from brain, heart, liver, lung, kidney, eye, pancreas and spleen of adult *Xenopus*. Total RNA was extracted from the tissues and converted to cDNA by reverse transcriptase reaction as described above. PCR was performed by the same method described above.

Whole-mount *in situ* hybridization

Whole-mount *in situ* hybridization (WISH) was performed using albino *Xenopus* embryos at stage 18 (middle neurula). Thirty embryos were fixed with fully dehydrated ethanol. A DNA fragment for the probe was constructed by primers 5 and 6. PCR was performed as follows: denaturation at 94^0C for 3 min, then 30 cycles of 94^0C for 1 min, 52^0C for 2 min, and 68^0C for 1 min. The amplified *Xenopus* sEH cDNA fragment included 887 bp nucleotides and was ligated into pBluescripIISK+ vector. The sense probe for sEH was prepared by linearization with *Hin*dIII and transcribed with T3 RNA polymerase. The anti-sense probe for sEH was prepared by linearization with *Bam*HI and by transcription with T7 RNA polymerase. This probe was hybridized and visualized according to the protocol for Roche Diagnostics DIG with minor modification [30,31]. Images of in situ hybridizations were taken using an Olympus SZX16 Stereo Microscope equipped with an Olympus DP71 microscope digital camera.

Isolation of *Xenopus sEH* cDNA and preparation of sEH mutant

Full-length *Xenopus sEH* cDNA was isolated by PCR using primers 7 and 8 in Table I-1. These primers were designed from the nucleotide sequence reported as *Xenopus sEH* (GenBank accession no. NM_001093674). PCR was

performed using cDNA synthesized from total RNA of *Xenopus* tailbud embryos (st.38) with GeneAmp high fidelity Taq DNA polymerase: denaturation at 94^0C for 3 min, then 30 cycles of 94^0C for 1 min, 55^0C for 2 min, and 68^0C for 1 min. The amplified *sEH* cDNA included 1683 bp nucleotides, from which the deduced protein had an open reading frame of 561 amino acid residues. The amino acid sequence deduced from the DNA sequence of the isolated *Xenopus sEH* cDNA in this study was found to have two amino acid substitutions, Thr to Asn at 29 and Arg to His at 146 (N29T/H146R), compared with the amino acid sequence of *Xenopus sEH* reported in GenBank (accession no. NM_001093674). The nucleotide sequences of several cDNAs from different individuals were analyzed and found to have same substitution. Therefore, it may be a native mutation. The clone of *Xenopus sEH* cDNA reported in GenBank was prepared by substitution of N29T/H146R.

Table I-1. Primers used in this study.

Primer No.	Sequences of primers
1	5'-CGGGATAACATTCAGGGTATCACT-3'
2	5'-ATCCATGGCGGTAACTGTCTTCCT-3'
3	5'-GGTTGTAGAGTCGTGTCGTA-3'
4	5'-CTCCAGGAATACCAACTCTC-3'
5	5'-GGAATTCCATATGGCTGGGAAGCGCTTCGT-3'
6	5'-AAGGATCCATGGCTTCCCAGAGAGTT-3'
7	5'-GGAATTCCATATGGCTGGGAAGCGCTTCGT-3'
8	5'-TGCAAGCTTCAGTTTGGATGTTACGGGCA-3'
9	5'-TTAATACGACTCACTATAGG-3'
10	5'-GGGAGATGTAGGCTAGTTTCTAGCCGTTGAA-3'
11	5'-TAGCCTACATCTCCCCAGTG-3'
12	5'-TCTGCAACAAACTTGGAGAA-3'
13	5'-TTCTCCAAGTTTGTTGCAGA-3'
14	5'-ACCAGGTCAAAATGGCGACTTAGTGAAGAGA-3'
15	5'-CCATTTTGACCTGGTTGTAG-3'
16	5'-CTCCAGGAATACCAACTCTC-3'
17	5'-TTAATACGACTCACTATAGG-3'
18	5'-CTCCAGGAATACCAACTCTC-3'
19	5'-GGGGTCCTGCTCACCCCTGGG-3'
20	5'-CTTCCAGGAATACCAACTCTC-3'
21	5'-TTAATACGACTCACTATAGG-3'
22	5'-TTCAATCAACGGAACTCCGGTCACTTTCTC-3'
23	5'-GAGAAAGTGACCGGAGTTCCGTTGATTGAA-3'
24	5'-TGATGATGATGCGGCCGCCAGTTTGGATGTTACGGGCAAGTTA-3'

Fragment I was amplified by PCR with primers 9 and 10 and fragment II with primers 11 and 12. Fragment III was amplified using primers 13 and 14. Fragment IV was amplified using primers 15 and 16. To obtain fragment V, fragments I and II was used as templates with primers 17 and 13. Fragment VI was made using fragments III and IV with primers 17 and 12. The last step was to obtain mutant 1 by fragments V and VI, used as templates with primers 18 and 12. By comparing our *Xenopus* sEH with human sEH, I found that Asp residues at 11 were substituted by Gly, which is an active site of phosphatase, and sEH G11D was designated xsEH mutant 2. PCR with primers 19 and 20 was carried out as above. A chimera, having a phosphatase domain of human sEH and epoxide hydrolase domain of *Xenopus* sEH, was also prepared. Primers for the phosphatase domain (primers 21 and 22) amplifies fragments corresponding to human sEH amino acids 1-334. Primers for epoxide hydrolase domain (primers 23 and 24) amplifies fragments corresponding to *Xenopus* sEH amino acids 334-563. To combine both of these domains, primers 21 and 24 were used to amplify fragments. All fragments were ligated into pET-21a(+) (Novagen).

Purification of *Xenopus* sEH

Full-length cDNAs of *Xenopus* wild-type, mutant 1, mutant 2 and chimera sEH were subcloned into pET-21a(+) vector with *Bam*HI and *Xba*I enzymes sites (Takara Bio, Shiga, Japan). The recombinant His-tagged sEH proteins expressed in *E. coli*, BL21-CodonPlus (DE3) (Stratagene, La Jolla, CA) were purified with a Ni-NTA agarose column (Qiagen, Hilden, Germany). The purified proteins were dialyzed in 10 mM Tris Buffer, pH 7.5, overnight and their concentrations were measured with the Bradford method (Protein Assay, Bio-Rad, Hercules, CA).

Assay of epoxide hydrolase activity

Epoxide hydrolase activity of sEH was measured using a fluorescent substrate, 3-phenyl-cyano (6-methoxy-2-naphthalenyl) methyl ester-2-oxiraneacetic acid (PHOME) purchased from Cayman Chemical (Ann Arbor, MI). Purified *Xenopus* sEH and human sEH (0.5 μg) were reacted with 25 μM PHOME in 25 mM Bis Tris-HCl, pH 7.0, containing 0.01% Bovine Serum Albumin (BSA). The effect of pH on EH activity was evaluated with Bis Tris buffer (pH 5.5-7.5). The effect of ionic strength was evaluated with 10, 25, 50, and 100 mM Bis Tris buffer (pH 7.0). The catalytic activity of purified *Xenopus* sEH and human sEH was investigated for temperatures ranging from 20 to 37^0C. For inhibition assay, *Xenopus* sEH or human sEH was incubated with 25 μM PHOME in 25 mM Bis Tris buffer, pH 7.0, containing 0.01% BSA in the absence or presence of 0 to 0.2 μM of *N, N'*-dicyclohexyl urea (DCU) (Wako, Osaka, Japan). Fluorescence of the reaction product, 6-methoxy-2-naphthaldehyde (6-MNA), was measured every 5 min for 60 min by the EnVision 2104 Multilabel Reader (Perkin Elmer, Waltham, MA) at an excitation wavelength of 330 nm and an emission wavelength of 465 nm at 30^0C. The concentration of 6-MNA produced by sEH was determined with a calibration curve prepared with authentic 6-MNA.

Assay of phosphatase activity

Phosphatase activity was measured using 4-Methylumbelliferyl Phosphate (Wako, Osaka, Japan) in 25 mM Bis Tris buffer, pH 7.0, containing 1 mM $MgCl_2$ and 0.01% BSA. The reaction was started by the addition of the enzyme, purified *Xenopus* sEH or human sEH (5.0 μg). The effects of ionic strength, pH and temperature were assessed as described above. The reaction was performed at 37^0C for up to 60 min and the fluorescence intensity of the produced 4-methylumbelliferone was measured every 5 min by the EnVision 2104 Multilabel Reader at an excitation wavelength of 330 nm and an emission wavelength of 465 nm.

Phosphatase assay of *Xenopus* sEH using malachite green

The phosphatase activity of sEH toward LPA (stearoyl L-**α-**lysophosphatidic acid (1-octadecanoyl-sn glycerol-3-phosphate) sodium salt) (Avanti Polar Lipids, Birmingham, AL) was detected by the Biomol green assay (Enzo Life Science, Plymouth Meeting, PA) according to the manufacturer's instructions. Arachidonoyl L-**α-**lysophosphatidic acid sodium salt and arachidoyl L-**α-**lysophosphatidic acid sodium salt were purchased from Echelon Bioscience (Salt Lake City, UT). Dipalmitoyl L-**α-**lysophosphatidic acid sodium salt was from Wako. Purified human sEH, *Xenopus* sEH, and chimera (0.6 μg) were pre-incubated for 5 min at 37^0C in 25 mM Bis Tris buffer, pH 7.0, containing 1 mM $MgCl_2$ and 0.01% BSA. LPAs were added at a final concentration of 10 μM and incubated for 5 min at 37^0C. The reaction was stopped by the addition of Biomol green reagent and held at room temperature for 60 min. The resulting green color was measured by the EnVision 2104 Multilabel Reader at 630 nm.

Separation and quantitation of EET metabolites

The epoxide hydrolase activities of purified recombinant *Xenopus* sEH, human sEH and chimera toward 10 μM EETs (11,12 EET or 14,15 EET) were assayed in incubation mixture (final volume 0.5 ml) consisting of 100 mM potassium phosphate buffer, pH 7.4, and 2 nmol stearic acid as an internal control. The reaction mixture containing purified recombinant protein (6.0 μg) was incubated at 37^0C for 5 min and the reaction was stopped by the addition of 0.4 M citric acid and I mL of ethyl acetate. After centrifugation at 4000 rpm for 10 min, the upper organic layer was transferred to a new tube and evaporated under nitrogen. The resulting residue was dissolved in ethanol (20 μl) and analyzed by HPLC equipped with an Evaporative Light Scattering Detector (ELSD) system (Prominence-Shimadzu, Kyoto, Japan) using a TSKgel ODS-100Z 5μm column (4.4 mm I.D x 15 cm; Tosoh, Tokyo, Japan). To detect

EET metabolites, mobile phase A (water: acetic acid, 100:0.1), and mobile phase B (acetonitrile: acetic acid, 100:0.1) were used. The metabolites were separated at a flow rate of 1 ml/min, with a linear gradient of A to B from 50% to 100% for 30 min. DHET production was measured by a calibration curve prepared with authentic DHETs.

Sample preparation and analysis of endogenous substrate

Eighty milligrams of *Xenopus* liver was homogenized and 200 µl of methanol and 2 µl of formic acid were added. The homogenates were centrifuged at 14,000 rpm for 10 min at 4^0C. The supernatants were applied to the SPE cartridge and washed with 3 ml of water, and 1 ml of 10% methanol. The sample was eluted in 0.5 ml acetonitrile followed by 1.5 ml ethyl acetate. These fractions were combined and dried under N_2 [32,33]. The residue was dissolved with 40 µl of ethanol for analysis by UPLC/electrospray ionization (ESI)/MS. The chromatography was performed with a C18 reversed-phase column (TSK-GEL ODS-140HTP, 4.6 x 250 mm, 5 µm) and the UPLC system (Acquity UPLC system, Waters, Milford, MA). Mobile phase A consisted of 50% water, 30% acetonitrile, 20% methanol and 1% acetic acid. Mobile phase B consisted of 80% acetonitrile, 20% methanol and 1% acetic acid. A flow rate of 0.2 ml/min and 5 µl injection volume was used to deliver the mobile phases A and B with a linear gradient from 40% A for 20 min to 40-100% B for 27 min. Mass spectrometry was carried out using a Nanofrontier LD mass spectrometer (Hitachi, Tokyo, Japan) and ESI. The analytes were detected by tandem TOF monitored by total ion, *m/z* 319 (EETs).

Statistics and kinetics analysis

The kinetic parameters *K*m and *V*max were obtained using Prism enzyme kinetic software (Graphpad Software, La Jolla, CA). Statistical analysis was performed with Student's *t*-test and $p<0.05$ were considered significant.

I.3 Results

Expression and purification of *Xenopus* sEH and its catalytic activity

I found two substitutions of amino acid in the sequence deduced from our *Xenopus* sEH cDNA compared with that of the original *Xenopus* sEH reported in GenBank. I prepared *Xenopus* sEH with substitutions of amino acid residues with N29T and H146R (designated mutant 1). Both amino acid exchanges occurred in the phosphatase domain. The purified *Xenopus* sEH was reacted with the generic substrate 4-Methylumbelliferyl Phosphate for phosphatase activity and with PHOME as a substrate for EH activity. The *Xenopus* sEH revealed significant EH activity (Fig. I-1A) but no phosphatase activity (Fig. I-1B). Also, another substrate for phosphatase, *p*-nitrophenyl phosphate, was used, but mutant 1 (N29T/H146R) and wild-type *Xenopus* sEH still had no phosphatase activity (data not shown).

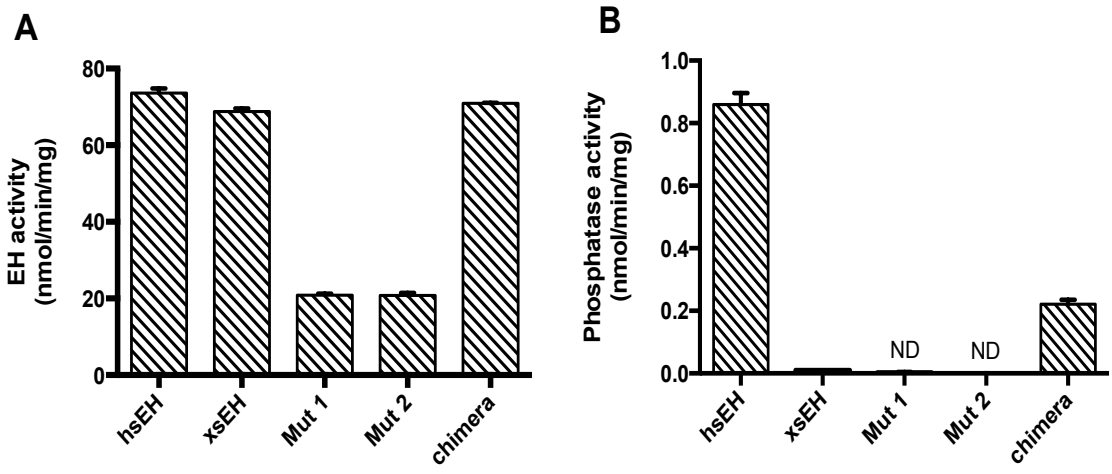

Fig. I-1 The epoxide hydrolase and phosphatase activities of *Xenopus* and human sEH. (A) EH activities of *Xenopus* wild-type, Mutant 1, Mutant 2, and Chimera sEH were assessed using purified protein (0.5 μg) toward 25 μM PHOME. (B) Purified sEH (5 μg) was incubated with 0.5 mM 4-Methylumbelliferyl Phosphate. The fluorescence of 4-methylumbelliferone was measured every 1 min for 60 min at 330 nm (exitation) and 465 nm (emission).

To investigate whether mutant 1 and wild-type *Xenopus* sEH lack phosphatase activity, a homology search of the phosphatase domain was performed with other members of haloacid dehalogenase (HAD), phosphonoacetaldehyde hydrolase (Phos), and phosphoserine phosphatase (PSP). Several amino acid residues have important functions in the two-step catalytic mechanism of phosphatase compared with HAD, Phos and PSP [34]. Based on the sequence homology with human sEH phosphatase domain, almost all residues important for phosphatase activity are conserved in *Xenopus* sEH, but the amino acid residue of the 11th aspartic acid was not conserved (Fig. I-2).

This amino acid residue is thought to be important for phosphatase activity. Wild-type *Xenopus* sEH has a glycine residue at the 11th position and sEH G11D (designated mutant 2) was constructed by exchanging the 11th glycine with aspartic acid. The EH activity of *Xenopus* sEH G11D was lower than that of human sEH, and *Xenopus* sEH G11D lacked phosphatase activity (Fig. I-1). These results suggest that other amino acid substitutions or regions of the peptide chain are required for phosphatase activity. The *Xenopus* sEH chimera was constructed by combining the human sEH phosphatase domain and *Xenopus* sEH epoxide hydrolase domain. The N-terminal domain of *Xenopus* sEH (1st to 232th amino acids) was exchanged for human sEH (1st to 229th amino acids). The EH activity of the chimera was measured and was found to be similar to that of wild-type *Xenopus* sEH. The chimera also had phosphatase activity, suggesting the C-terminal domain of *Xenopus* sEH was not a cause of the lack of phosphatase activity (Fig. I-1B).

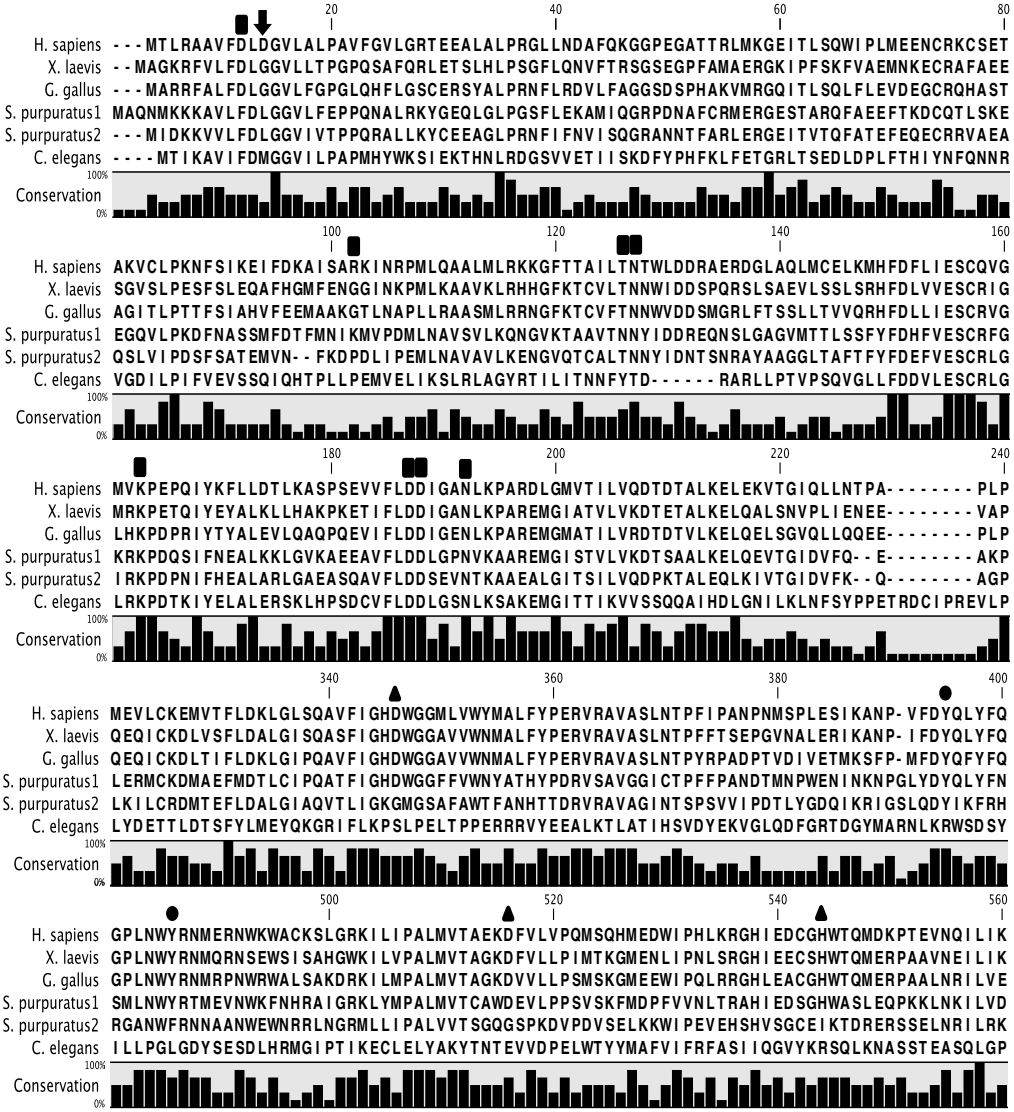

Fig. I-2 Sequence alignment between *Xenopus* sEH and sEH derived from other species. Black boxes indicate the active sites of phosphatase activity. The arrow indicates a different amino acid of phosphatase active site between human and *Xenopus* sEH. Thr27 or Arg146 indicated by open circle was substituted by Asn or His, respectively, in the isolated *Xenopus* sEH.

Xenopus sEH activity toward endogenous substrates

To investigate the EH activity of *Xenopus* sEH toward the endogenous substrates, 11,12-EET and 14,15-EET, the metabolized DHETs were analyzed

by the HPLC-ELSD system. The activity of *Xenopus* sEH toward 11,12-EET was not different from that of hsEH or chimera (Fig. I-3A). Consequently, the activities of *Xenopus* sEH and chimera toward 14,15-EET were not significantly different from that of human sEH (Fig. I-3B). Recently, we found that LPAs were substrates for phosphatase activity [4]. Human sEH had phosphatase activity toward LPAs, but *Xenopus* sEH did not (Fig. I-3C).

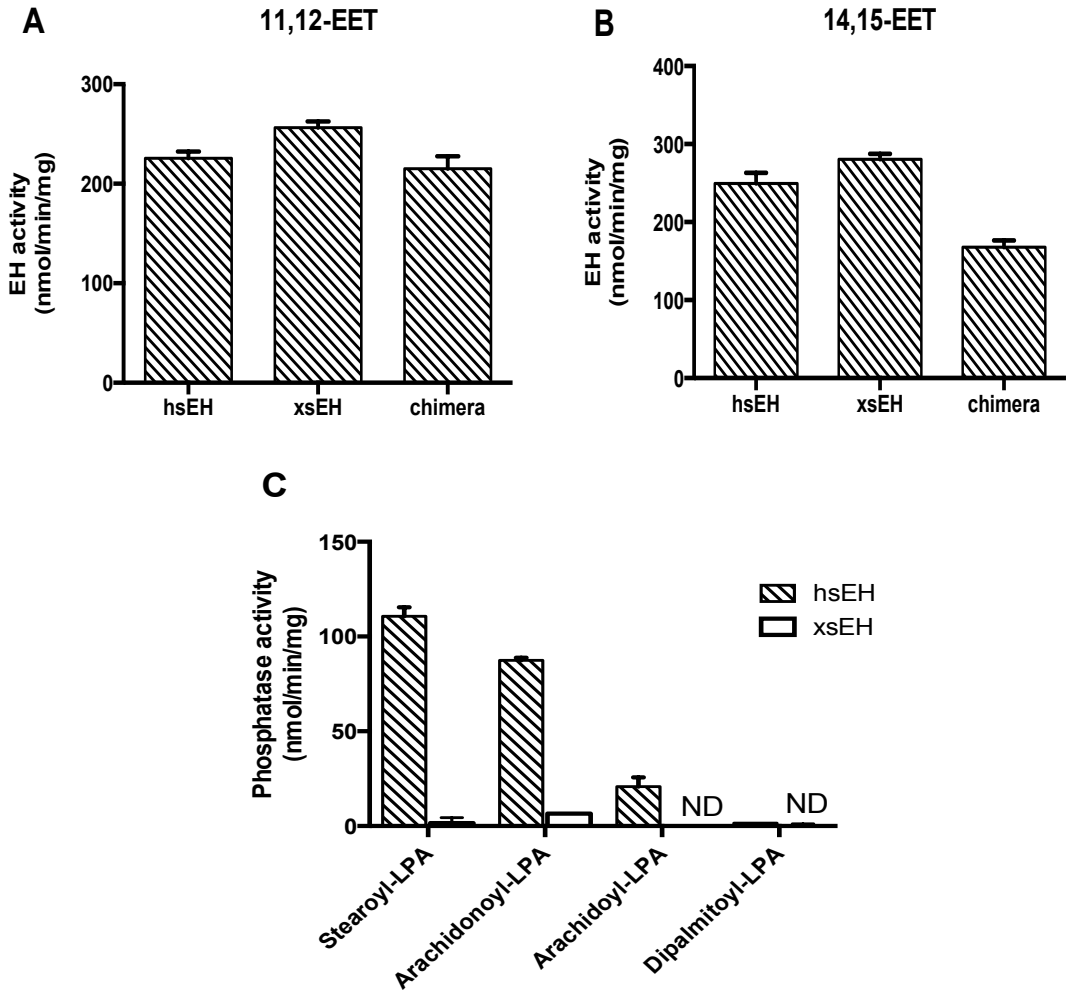

Fig. I-3 EH activities of *Xenopus*, human and chimera toward 11,12-EET, 14,15-EET and their phosphatase activities toward LPAs. (A and B) purified *Xenopus,* human or chimera sEH (6 μg) was incubated with 10 μM 11,12 EET (A) or 14,15 EET (B) at 37°C for 15 min then analyzed by HPLC-ELSD. (C) Purified human sEH, or *Xenopus* sEH (0.6 μg) was incubated with 10 μM stearoyl-LPA, arachidonoyl-LPA, arachidoyl-LPA, and dipalmitoyl-LPA, and the phosphatase activities were detected by malachite green. Results are expressed as the mean ± SD of three separate experiments.

Epoxide hydrolase and phosphatase assay in various conditions

Ionic strength and pH of buffer, and reaction temperature were assessed to determine the optimal condition for both EH and phosphatase activity.

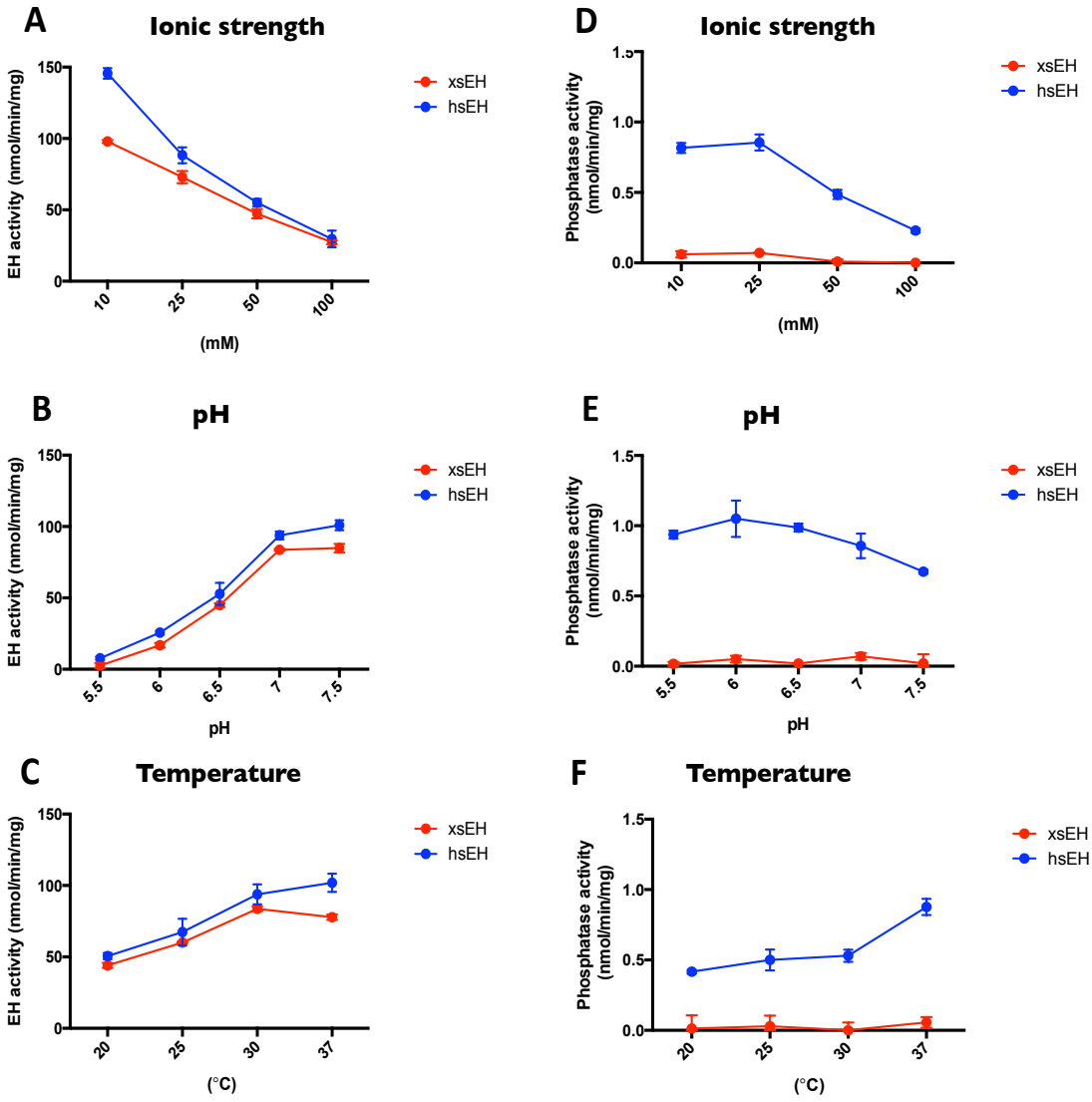

Fig. I-4 The effect of ionic strength and pH of buffer, and reaction temperature on catalytic activities of *Xenopus* and human sEH. (A) Purified *Xenopus* sEH or human sEH (0.5 μg) was incubated with 25 μM PHOME with 10, 25, 50, or 100 mM Bis Tris buffer pH 7.0 at 30^{0}C. (B) EH activities toward 25 μM PHOME in 25 mM Bis Tris buffer, pH 5.5, 6.0, 6.5, 7.0, or 7.5 at 30^{0}C (C) EH activity in 25 mM Bis Tris buffer pH 7.0 at 20, 25, 30, or 37^{0}C. (D-F) Purified sEH (5 μg) were each incubated with 0.5 mM 4-Methylumbelliferyl Phosphate in the various conditions descrived above.

The pH and ionic strength of buffer was evaluated with 10-100 mM Bis Tris buffer, pH 5.5-7.5, at the different temperature from 20 to 37^{0}C. *Xenopus* sEH revealed maximal EH activity in 10 mM Bis Tris buffer, pH 7-7.5, at 30^{0}C, while human sEH showed maximal EH activity in 10 mM Bis Tris buffer, pH 7-7.5, at 37^{0}C (Figs. I-4A; B; C). In the phosphatase activity of human sEH, maximal activity was obtained in 25 mM Bis Tris buffer, pH 6.0, at 37^{0}C (Figs. I-4D; E; F). However, *Xenopus* sEH did not show phosphatase activity under these conditions.

The EH activity of *Xenopus* and human sEH were assessed in the presence of a selective EH inhibitor, *N, N'* Dicyclohexylurea (DCU) [35]. DCU efficiently inhibited the EH activities of *Xenopus* and human sEH at a concentration of 50 nM (Fig. I-5A). The EH activities of *Xenopus* and human sEH were detected using PHOME, and *K*m and *V*max were determined. The *Xenopus* sEH had higher *K*m (19.16±7.64 μM) and lower *V*max (147.08±30.2 nmol.min^{-1}.mg^{-1}) than that of human sEH, with *K*m (17.27±5.31) and *V*max (227.42±36.6 nmol.min^{-1}.mg^{-1}) (Figs. I-5B; C).

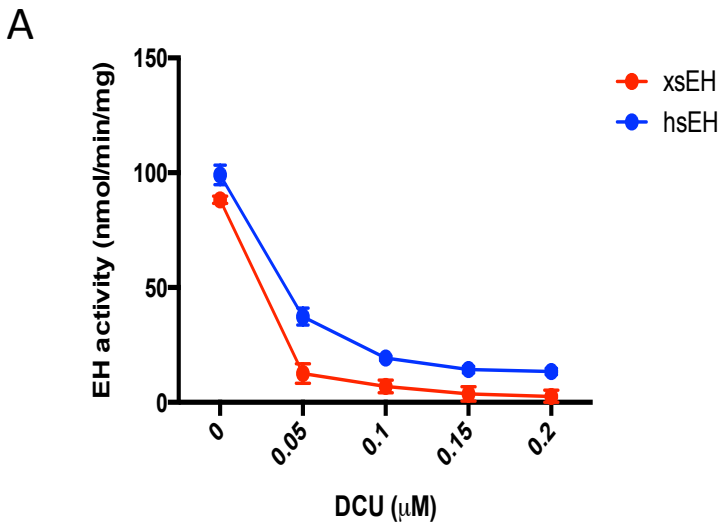

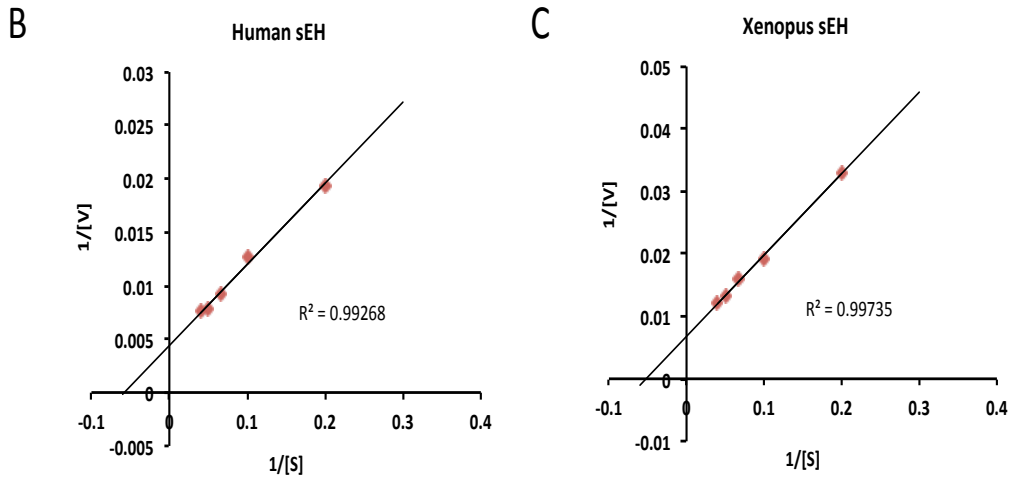

Kinetic parameter	Human	Xenopus
Km (μM)	17.27 ± 5.31	19.16 ± 7.64
Vmax (nmol/min/mg)	227.42 ± 36.3	147.08 ± 30.2

Fig. I-5 Inhibition of EH activity by DCU and kinetic analysis of EH activity.
(A) Purified *Xenopus* sEH or hsEH (0.5 μg) was incubated with 25 μM PHOME in the presence of 0.0-0.2 μM DCU. (B, C) Lineweaver-Burk plots of the epoxide hydrolase activities toward PHOME and the kinetic parameters were obtained using Graphpad Prism enzyme kinetic software. Results are expressed as the means ± SD of triplicate experiments.

Presence of EETs in *Xenopus* liver

EETs production in the *Xenopus* liver as an endogenous substrate of sEH was characterized (Fig. I-6). The endogenous EETs were measured by LC-MS. Peaks of 11,12-EET, 14,15-EET were detected, and the addition of authentic 11,12-EET, 14,15-EET increased the peak height, suggesting that 11,12-EET and 14,15-EET were present in the *Xenopus* liver.

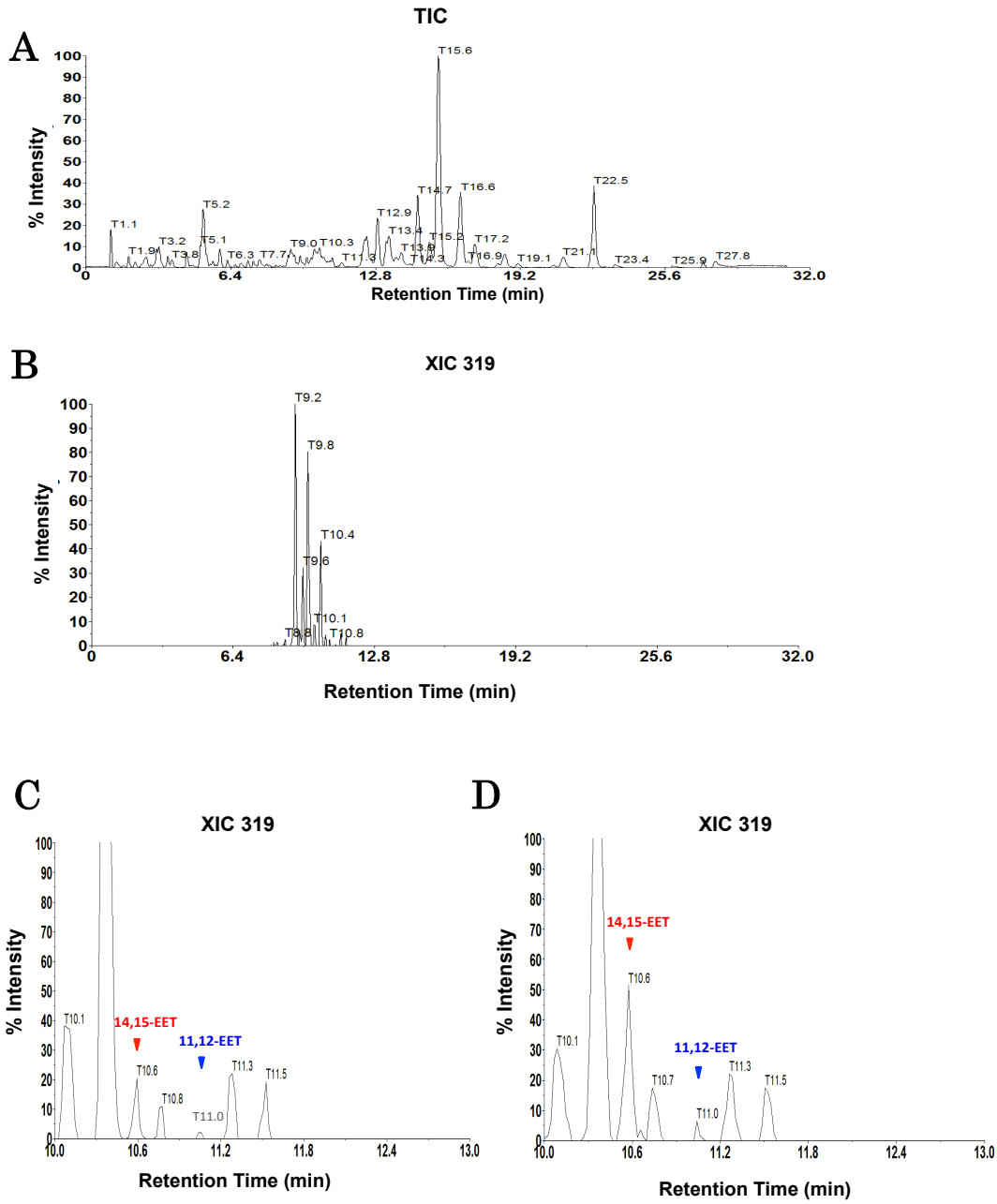

Fig. I-6 Detection of 11,12-EET and 14,15-EET in *Xenopus* liver by LC-MS.
Xenopus liver (80 mg) were homogenized and analyzed by UPLC/ESI/MS. (A) The total ion chromatogram of *Xenopus* liver (B, C) the selected ion chromatogram with *m/z* 319 (EETs). (D) Selected ion chromatogram with *m/z* 319 of *Xenopus* liver by addition of authentic 11,12-EET and 14,15-EET (0.4 pmol). TIC, total ion chromatogram; XIC, extracted ion chromatogram.

RNA and protein levels of *Xenopus* sEH during embryonic development

sEH mRNA levels in *Xenopus* embryos were investigated by RT-PCR. Embryos from 0 stage (0 time after fertilization) until 38 stages (tailbud) showed a clear band, and mRNA levels were increased with aging or the development of embryos (Fig. I-7A). The expression of sEH protein in embryos at various stages was investigated. The cytoplasmic layer of embryos was subjected to SDS-polyacrylamide gel electrophoresis and immunoblotting. The protein level of xsEH was consistent with the RNA level (Fig. I-7B).

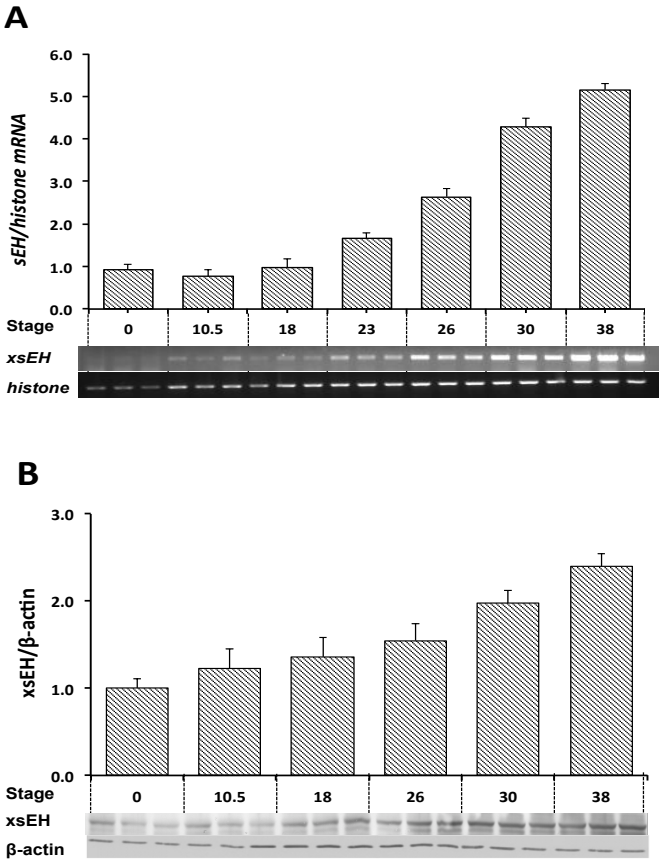

Fig. I-7 The mRNA and protein levels of *Xenopus* sEH in embryos.
(A) *Xenopus sEH* mRNA levels were detected at the stages 0, 10.5, 18, 23, 26, 30, and 38 of *Xenopus* embryo. Total RNA was isolated from embryos and RT-PCR was performed. Amplified DNA fragments were analyzed by electrophoresis with 2% agarose gel. The ratio of *Xenopus sEH* mRNA/*histone-H4* in the stage 0 was set at 1. The values on the graphs are the means ± SD of three separate samples. Band intensity was measured by NIH image and normalized to that of *histone-H4*. (B) xsEH

protein levels in *Xenopus* embryos were detected by Western blotting. Ten embryos were homogenized and separated into three distinct layers: lipid, cytoplasmic, and pigment granule/yolk. The cytoplasmic layer (30μg protein) was subjected to SDS-polyacrylamide gel electrophoresis and analyzed by western blotting with the antibody against human sEH or β-actin. *Xenopus* sEH protein levels were normalized by expression level of β-actin protein. The ratio of *Xenopus* sEH protein/ β-actin in the stage 0 was set at 1. The values on the graphs are the means ± SD of three separate samples.

Expression of *Xenopus* sEH in various tissues and localization of *sEH* mRNA in the embryo by WISH

To investigate the distribution of *Xenopus* sEH in various tissues, total RNAs were extracted from adult *Xenopus*. RT-PCR was then performed on brain, heart, liver, lung, kidney, eye, pancreas and spleen (Fig. I-8). The highest expression was detected in the liver, with the lowest expression in the brain. The localization of *Xenopus sEH* mRNA in embryos was investigated by WISH at stage 30, the middle tailbud stage (Fig. I-9). The accumulation of *Xenopus sEH* mRNA was detected almost totally in the head region. The localization of *Xenopus* sEH was observed in the olfactory placode, cement gland, heart, pharyngeal cavity, eye vesicle, otic vesicle, and notochord.

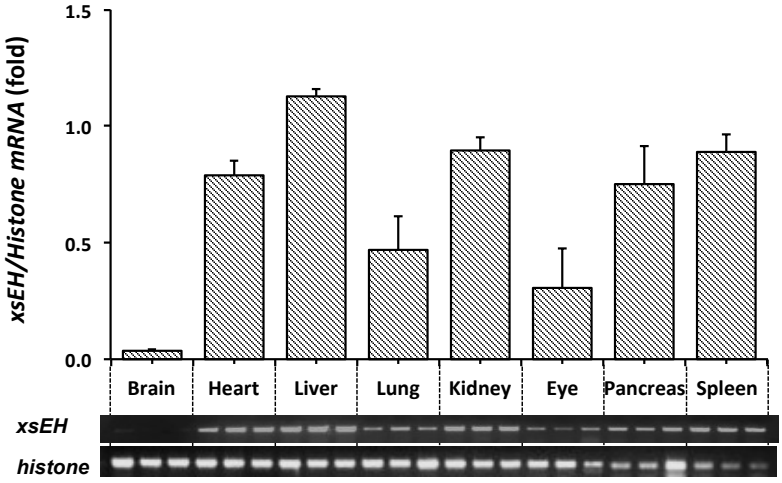

Fig. I-8 *sEH* mRNA distribution in several tissues of *Xenopus laevis*.
Total RNA was isolated from the brain, heart, liver, lung, kidney, eye, pancreas, and spleen and converted to cDNA. The amplified DNA fragments were run on an agarose gel (1%) and visualized with ethidium bromide staining. The band intensity of sEH

was quantified using NIH Image and normalized by *histone-H4*. The values on the graphs are the means ± SD of three separate samples.

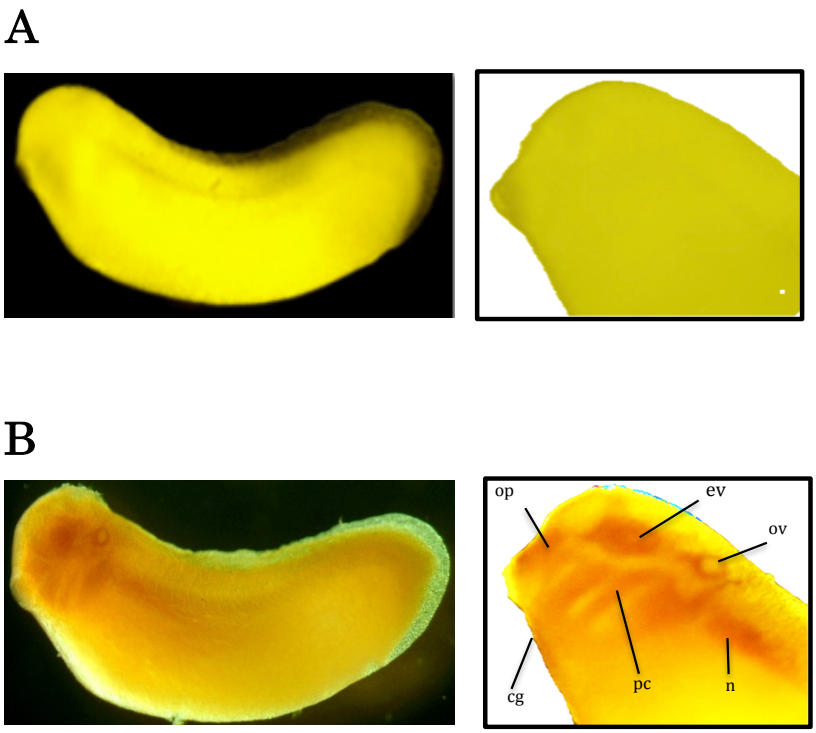

Fig. I-9 Localization of *Xenopus* sEH by WISH.
(A and B) Embryos were hybridized by a sense probe (A) and an antisense probe (B). The localization of *Xenopus* sEH was detected in the head region in olfactory placode (op), cement gland (cg), pharyngeal cavity (pc), eye vesicle (ev), otic vesicle (ov), and notochord (n).

I.4 Discussion

I isolated *Xenopus sEH* cDNA in this study. The sequence homology of *Xenopus* sEH compared with human sEH was high in the C-terminal region (65%). The amino acid residues forming the catalytic triad of the EHs were first identified from sequence alignment with the sequence of haloalkane dehalogenase [25,36]. The role of this residue is nucleophilic attack to the epoxide ring [37]. The catalytic triad of rat sEH is composed of three active sites residues: Asp333, Asp495 and His523 [38]. In human sEH, the catalytic triad is represented by Asp335, Asp496, and His524 (triangles on Fig. I-2). These residues also aligned in the *Xenopus* sEH, spaced over Asp336, Asp503, and His531. Two tyrosines (Tyr382 and Tyr465) polarized the epoxide in the human enzyme (circles on Fig. I-2) [39]. These residues and their approximate spacing are also conserved in the *Xenopus* sEH enzyme as Tyr385 and Tyr472, respectively.

Most amino acid residues were important for the phosphatase activity of human sEH (squares in Fig. I-2) were conserved in *Xenopus* sEH. Aspartic acid at the 11th position (arrow in Fig. I-2) is believed to be involved in the coordination of the Mg^{2+} atom in the active site while participating in a hydrogen bond with arginine at the 99th position [22]. This aspartic acid is missing in the *Xenopus* sEH as well as in chicken and purple sea urchin homolog (*Xenopus laevis,* GenBank accession no. NM_001093674). I prepared *Xenopus* sEH mutant 2 (G11D) with a single amino acid substitution at Gly11 (G11D), which seems to be important for phosphatase activity. Unexpectedly, *Xenopus* sEH G11D did not show phosphatase activity. However, the chimera consisting of the human N-terminal phosphatase domain and the *Xenopus* C-terminal EH domain displayed activity when assayed with 4-Methylumbelliferyl Phosphate. This result showed that the *Xenopus* C-terminal EH domain did not affect the N-terminal phosphatase domain.

The mammalian sEH catalyzes the hydrolysis of aliphatic epoxides such as EETs to their corresponding diols, DHETs. Recently, Zebrafish [3], chicken [7], and purple sea urchin [40] have been found to produce DHET. These findings raise the question of whether there is a sEH homolog in *Xenopus* with epoxide hydrolase activity similar to those of the mammalian enzymes. The discovery of a sEH homolog would have implications for developmental studies. In mammals, sEH is expressed in almost every organs, including the liver, lung, kidney, heart, brain, and ovary [5]. The enzyme is mainly localized in the cell cytosol, but sEH in some cell types shows dual localization, both cytosolic and peroxisome. From the results of this study, we conclude that *Xenopus* sEH was distributed in several tissues and organs widely although their levels of protein were differed. The characterization and distribution of sEH in *Xenopus embryos* has not been previously reported.

In conclusion, the homology in the amino acid sequence between human and *Xenopus* sEH is not high (56.2%). Human sEH has both EH and phosphatase activity, whereas *Xenopus* sEH does not have phosphatase activity at least toward several phosphatase substrates. This is important knowledge and a useful tool for further investigation of sEH in development.

CHAPTER II

The metabolism of lysophosphatidic acids by allelic variants of human soluble epoxide hydrolase

II.1 Introduction

Lysophosphatidic acids (LPAs) are phospholipids that act as important signaling molecules [41] and have been shown to function as substrates for the N-terminal domain of the human soluble epoxide hydrolase (sEH) [4,42]. LPA signaling contributes to a range of diseases, including neuropathic pain [43], cardiovascular diseases [17], cancer [44], fibrosis [45], infertility [46], and obesity [47]. The involvement of LPAs in signaling processes such as inflammatory response [48] and cell proliferation [49] suggests that these molecules would be good drug targets for the treatment of human diseases.

sEH is an enzyme with multiple biological functions and is involved in the metabolism of xenobiotics. The C-terminal domain of sEH catalyzes the hydrolysis of epoxides to their corresponding diols. Epoxides can be generated via oxidation of olefin or aromatic hydrocarbon by cytochrome P450s. sEH is present in the cytosolic and peroxisome fractions of the cell [50] and has a broad distribution in human tissues [51] The endogenous substrates of sEH are epoxyeicosatrienoic acids (EETs). EETs play roles in the anti-inflammatory properties of endothelial cells [52], vasodilation [53], and cell proliferation [54] and sEH plays an important role in their proper functioning.

A single nucleotide polymorphism (SNP) variants of sEH have been identified, and several allelic variants of sEH have been shown to exhibit different epoxide hydrolase activities [9,10]. In human sEH, six allelic variants, K55R, R103C, C154Y, R287Q, V422A, and E470G, were identified. [9] With respect to phosphatase activity, Morisseau et al. showed that the sEH variant R287Q exhibited lower activity toward myristoyl-LPA than the wild-type (WT) [55]. However, the effect of allelic variants of human sEH on the phosphatase activities toward other LPAs remains unknown. The R103C amino acid substitution was associated with increased induction of cell death in cortical neurons in response to oxygen-glucose deprivation and re-

oxygenation [13]. The R287Q was associated with increased plasma cholesterol levels in familial hypercholesterolemia [14] and with the onset on coronary artery calcification in Africa-American subjects [15]. R287Q has also been associated with insulin resistance in type 2 diabetic patients [16]. In addition, in human, the individuals which have a Lys55Arg variant have a higher risk of coronary heart diseases [56].

LPAs have been shown to function as substrates for the N-terminal phosphatase domain of sEH [4,42]. The functions of the phosphatase activities of sEH have been shown to include argumentation of the cholesterol synthesis in HepG2 cells [57]. In addition, we previously found that the phosphatase activity of sEH suppressed VEGF levels and cell growth in Hep3B cells [19]. In peritoneal mesothelial cells, LPA has been shown to induce VEGF expression in a concentration dependent manner [58]. Phosphatase activity of sEH has been linked to VEGF expression, but there is no evidence of physiologically relevant of allelic variants of sEH in VEGF expression. An examination of the actions of allelic variants of sEH on LPA hydrolysis could reveal other biological functions associated with the phosphatase activity.

In this study, I examined the mutated residues of sEH allelic variants to understand the effect of these variants on the metabolism of LPAs. These investigations may be useful for further clarifying the role of sEH allelic variants in regulating the hydrolysis of LPAs *in vivo*.

II.2 Materials and Methods

Materials

Stearoyl L-α-lysophosphatidic acid (1-octadecanoyl-sn glycero-3-phosphate) sodium salt (s-LPA) was purchased from Avanti Polar Lipids (Birmingham, AL), arachidonoyl L-α-lysophosphatidic acid sodium salt (arachidonoyl-LPA) and arachidoyl L-α-lysophosphatidic acid (arachidoyl-LPA) were obtained from Echelon Biosciences Inc. (Salt Lake, UT), geranylgeranyl pyrophosphate ammonium salt (GGPP) was obtained from Sigma Chemical (St. Louis, MO), and sphingosine-1-phosphate (S1P) was kindly provided by Professor Katsumura of Kwansei Gakuin University. 3-phenyl-cyano (6-methoxy-2-napthalenyl) methyl ester-2-oxiraneacetic acid (PHOME) was purchased from Cayman Chemical (Ann Arbor, MI). Trans-stilbene oxide (t-SO) was obtained from Acros Organics (Fair Lawn, NJ). 4-methylumbelliferyl phosphate (4-MUP) was obtained from Wako Pure Chemicals (Osaka, Japan).

Preparation of the constructs of allelic variants of sEH for expression in *E. coli*

The human WT and N-terminal domain (amino acids 1-221) of sEH in pET21a vector were constructed as described previously.[4)] The primers used in this study are shown in Table II-1. For the construction of sEH variants, the first half fragment was amplified with the primer sets 1 and 2 (K55R), 1 and 3 (R103C), 1 and 4 (C154Y), 1 and 5 (R287Q), 1 and 6 (V422A), and 1 and 7 (E470G), and the latter half fragment was amplified with the primer sets 8 and 9 (K55R), 8 and 10 (R103C), 8 and 11 (C154Y), 8 and 12 (R287Q), 8 and 13 (V422A), and 8 and 14 (E470G) using WT sEH cDNA as a template. The full-length of each variant was amplified with the primers 1 and 8 using fragments of the first half and the latter half as a template, and inserted into the pET21a vector with *Nde*I and *Xho*I sites.

TABLE II-1. Primers used in this study

No.	Sequences	
1	5'-GGAATTCCATATGACGCTGCGCGCGGCCGT-3'	Forward primer: 1st-20th nucleotides; the *Nde*I site is underlined and the start codon is double-underlined
2	5'-AGTGTGATCTCTCCTCTCATAAGCCGGGTAG-3'	Reverse primer: 149th-179th nucleotide; mutation T to C is underlined
3	5'-CCTGGAGCATGGGGCAGTTGATCTTTCTGGC-3'	Reverse primer: 292nd-322nd of nucleotide; mutation of G to A is underlined
4	5'-ACCATTCCCACCTGATACGACTCTATCAGGA-3'	Reverse primer: 446th-476th nucleotide; mutation of C to T is underlined
5	5'-GGTAACCTGCCTGGGCCAGA-3'	Reverse primer: 840th-859th nucleotide
6	5'-CTTTATGCATGGATAAAAC-3'	Reverse primer: 1246th-1264th nucleotide
7	5'-CCATGTTTCGGTACCAGTTT-3'	Reverse primer: 1389th-1408th nucleotide
8	5'-ATACTCGAGCATCTTTGAGACCACCGGTG-3'	Reverse primer: 1646th-1665th nucleotide; *Xho*I site is underlined
9	5'-AGGAGAGATCACACTTTCCC-3'	Forward primer: 165th-184th nucleotide
10	5'-CCCCATGCTCCAGGCAGCTC-3'	Reverse primer: 309th-328th nucleotide
11	5'-CCAGGCAGGTTACCAGGTCCTAGCTATGGA-3'	Forward primer: 846th-875th nucleotide; mutation of G to A is underlined
12	5'-TCAGGTGGGAATGGTCAAAC-3'	Forward primer: 462nd-481st nucleotide
13	5'-TATCCATGCATAAAGCCTGTGAAGCGGGAGG-3'	Forward primer: 1249th-1280th nucleotide; mutation of T to C is underlined
14	5'-GGTACCGAAACATGGGAAGGAACTGGAAGTG-3'	Forward primer: 1394th-1424th nucleotide; mutation of A to G) is underlined
15	5'-ATAGCGCGCGACCTCTTGCAATCCAAGTG-3'	Forward primer: 686th-706th nucleotide; *Bss*HII site is underlined
16	5'-AAACTCGAGAAGCTGGATTCCGGTCACTT-3'	Reverse primer: 644th-663th nucleotide; *Xho*I site is underlined

For construction of the C-terminal domain of sEH (amino acids 230-555), the fragment was amplified with the primers 15 and 16, and connected after the N-terminal 1st-5th amino acids of sEH with a *Bss*HII site. The N-terminal allelic variants of sEH (N-K55R, N-R103C, N-C154Y) were amplified with the primers 1 and 16 using each allelic variant of full-length sEH as a template, and inserted into the pET21a vector. The C-terminal allelic variants of sEH in the pET21a vector (C-R287Q, C-V422A, and C-E470G) were prepared by insertion of the mutation into the C-terminal domain of sEH in the same way as for the full-length variants of sEH. The WT and all variants of the sEH protein were expressed in *E. coli* (BL21(DE3)codon+) for 24 h at 25^0C. The proteins were purified with an Ni-NTA agarose column (Qiagen, Hilden, Germany) according to the manufacturer's instructions. The purified proteins were dialyzed against 50 mM Tris-HCL buffer, pH 7.5.

Cell culture and expression

The full-length WT or allelic variants of sEH (WT, K55R, R103C, C154Y, R287Q, V422A, and E470G) were ligated into *Bam*HI/*Eco*RI sites of the pcDNA3.1(+) vector (Invitrogen). The pcDNA plasmids containing sEH allelic variants were transfected into Hep3B cells, and the transfected cells were selected by G418. Total RNA was extracted from cells with Isogen (Nippongene, Toyama, Japan) according to the manufacturer's instructions, and converted to cDNA by reverse-transcription using RevertAid reverse transcriptase (Thermo, Pittsburgh PA, USA). Real-time PCR was performed with SYBR premix Ex Taq II (Takara, Shiga, Japan) following the manufacturer's instructions. PCR was performed using a Thermal Cycler Dice Real Time System Single TP850 (Takara, Shiga, Japan). The primers for human *VEGF* (Acc No. NM_ AF022375) were 5'-TTCATGGATGTCTATCAGCG-3' (forward) and 5'-CATCTCTCCTATGTGCTGGC-3' (reverse). The primers for human *histone-H4* (Acc No. NM_003548) were 5'-

TATCGGGCTCCAGCGGTCATGTC-3' (forward) and 5'-GGATCGAAACGTGCAAAGCTGGAG-3' (reverse).

Phosphatase activity assay and kinetics

Phosphate release was detected by the Biomol green assay. The Biomol green assay kit was purchased from Enzo Life Sciences (Plymouth Meeting, PA) and the assay was performed according to the manufacturer's instructions. Purified human sEH allelic variants (9.5 pmol) were pre-incubated for 5 min at 37^0C in 25 mM Bis Tris-HCl buffer, pH 7.0, containing 1 mM $MgCl_2$ and 0.01% Bovine Serum Albumin (BSA). Each substrate was added at the final concentration of 10 μM and incubated for 5 min at 37^0C. The reaction was stopped by the addition of Biomol green reagent and held at room temperature for 60 min. The resulting green color was measured by an EnVision 2104 Multilabel Reader (Perkin Elmer, Foster City, CA) at 630 nm. For comparison with the synthetic substrate, phosphatase activity was measured using 4-MUP in 25 mM Bis Tris-HCl buffer, pH 7.0, containing 1 mM $MgCl_2$ and 0.01% BSA. Purified full-length sEH (80 pmol) or N-terminal domain variants (80 pmol) were used. The reaction was started by addition of 4-MUP at a concentration of 0.5 mM. The reaction was performed at 37^0C for up to 60 min and the fluorescence intensity of the produced 4-methylumbelliferone was measured every 5 min by an EnVision 2104 Multilabel Reader at an excitation wavelength of 330 nm and emission wavelength of 465 nm. For the determination of kinetic parameters of sEH variants, phosphatase activities toward stearoyl-LPA (final concentration: 2, 4, 8, 15 and 20 μM) were measured, and the *K*m and *V*max were obtained using Prism Graphpad enzyme kinetic software as described previously [4].

Epoxide hydrolase activity assay

Epoxide hydrolase activities of the full-length and C-terminal allelic variants of sEH were measured with a fluorescent substrate, PHOME [59]. The

full-length (1.6 pmol) and C-terminal domain (1.6 pmol) of sEH were reacted with 25 μM PHOME in 25 mM Bis Tris-HCL buffer, pH 7.0, containing 0.01% BSA at 30^0C. The reaction mixture was analyzed by an Envision 2104 Multilabel Reader every 1 min for 30 min at an excitation wavelength of 330 nm and emission wavelength of 465 nm. The fluorescence intensity of the reaction product, 6-metoxy-2-naphthaldehyde (6-MNA), was determined with a calibration curve prepared with the authentic 6-MNA. The epoxide hydrolase activities of the full-length variants and C-terminal variants of sEH were also measured using *t*-SO as a substrate by HPLC. The purified proteins of the full-length variants (0.48 nmol) and C-terminal variants (0.48 nmol) of sEH were incubated with *t*-SO (50 μM) in 25 mM Bis Tris-HCl buffer (pH 7.0) containing BSA (0.1 mg/ml) for 15 min at 37^0C. The enzymatic reaction was stopped by addition of ethyl acetate (1 ml). After centrifugation at 4,000 rpm for 10 min, the upper organic layer was transferred to a new tube and evaporated under nitrogen. The resulting residues were dissolved in 75% methanol and analyzed by HPLC using a TSKgel ODS-100V (4.6 mm I.D. x 15 cm; Tosoh, Tokyo, Japan). To detect *t*-SO metabolites, mobile phase A (water: acetic acid, 100:0.1) and mobile phase B (acetonitrile: acetic acid, 100:0.1) were used. The HPLC was run at a flow rate of 0.7 ml/min, with a linear gradient from 30% A to 100% B for 30 min. The amount of produced *t*-SO diol was determined with a calibration curve prepared with the authentic *t*-SO diol (Sigma-Aldrich, St. Louis, MO).

Statistical analysis

All experiments were repeated at least three times with three replicates in each experiment. A Student's *t*-test was used for comparing the levels of each activity.

II.3 Results

Epoxide hydrolase activity of sEH allelic variants

The epoxide hydrolase activities of the WT and allelic variants of sEH toward *t*-SO were measured (Fig. II-1A). All allelic variants of full-length sEH showed epoxide hydrolase activity similar to that of the WT sEH. Next, I investigated the activities of the allelic variants in the separated C-terminal domain of sEH, because the N-terminal and C-terminal domains of sEH have respective phosphatase and epoxide hydrolase activities independently, and large effects of the substitution on the activity of C-terminal domain were expected compared with that of full-length.

A

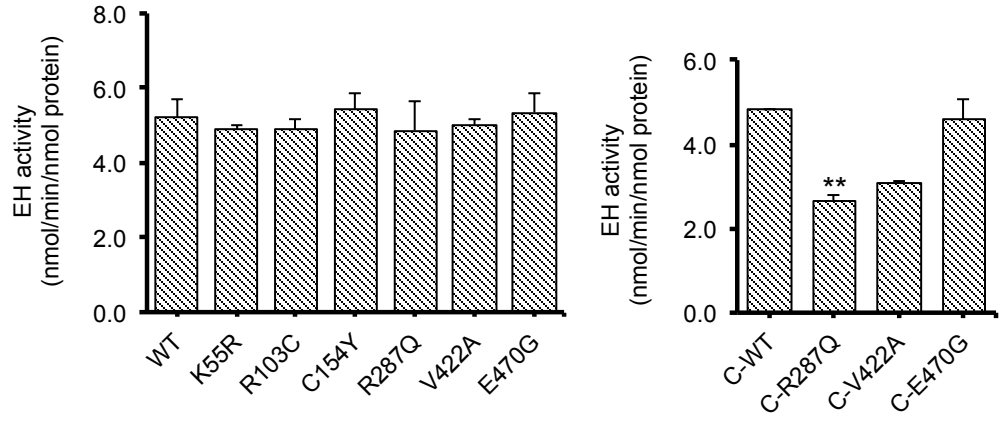

B

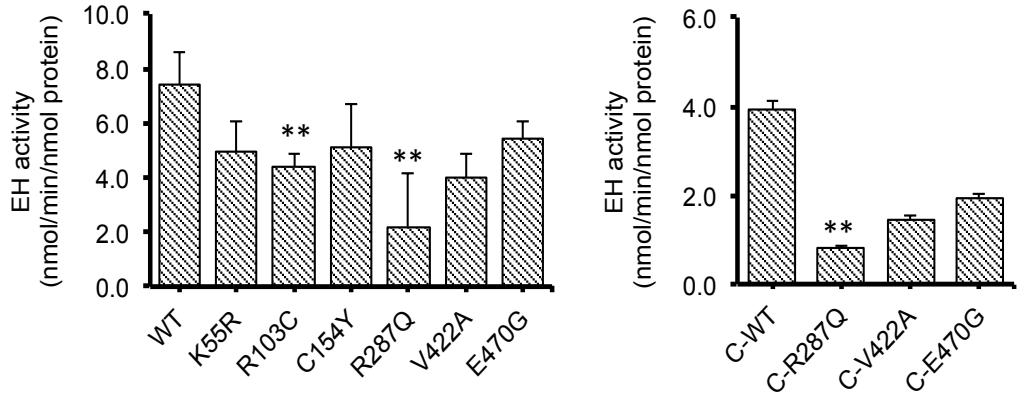

Fig. II-1 Epoxide hydrolase activities of sEH allelic variants toward *t*-SO and PHOME. (A) The full-length (0.48 nmol) and C-terminal domain (0.48 nmol) of sEH allelic variants purified protein were reacted with *t*-SO (50 μM) at 37^{0}C for 15 min, then analyzed by HPLC. (B) The full-length (1.6 pmol) and C-terminal domain (1.6 pmol) of sEH allelic variants were reacted with PHOME (25 μM) at 30^{0}C. EH, epoxide hydrolase. Values are given as the mean for three replicate experiments. ***p*<0.01, significantly different from WT sEH.

As a result, the C-terminal allelic variant C-R287Q showed significantly lower activity than that of the WT C-terminal domain of sEH. On the other hand, the epoxide hydrolase activities of the full-length R103C and R287Q toward PHOME were lower than that of the WT (Fig. II-1B). C-R287Q also showed significantly lower activity than that of the WT.

Phosphatase activity of sEH allelic variants toward 4-MUP

The phosphatase activities of sEH allelic variants toward synthetic substrate, 4-MUP, were investigated (Fig. II-2). I found that the full-length R103C and R287Q displayed significantly lower activity than the WT. On the other hand, the N-terminal allelic variants, N-K55R, N-R103C, and N-C154Y showed lower activity than the WT N-terminal domain of sEH.

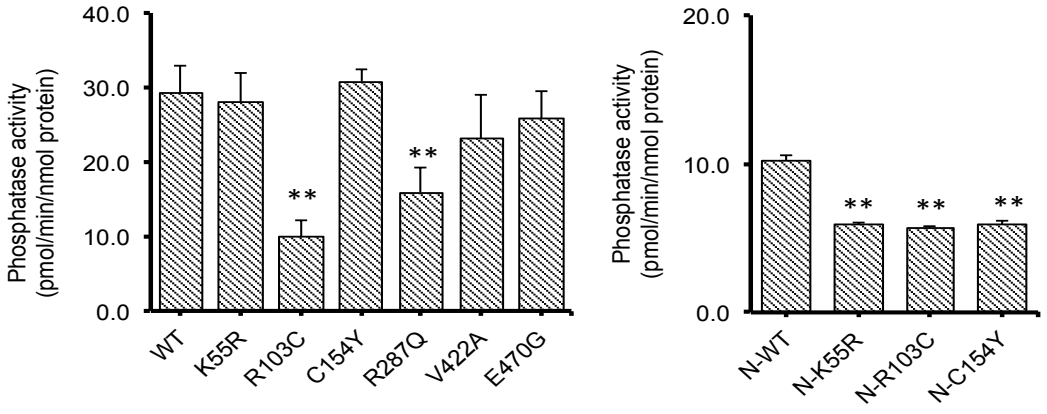

Fig. II-2 Phosphatase activities of sEH allelic variants toward 4-MUP.
Full-length and N-terminal domain of sEH allelic variants (80 pmol) were incubated with 4-MUP (0.5 mM), and the fluorescence of the hydrolyzed product was measured every 1 min for 60 min at 330 nm (Ex) and 465 nm (Em). Values are given as the mean for three replicate experiments. ***p*<0.01, significantly different from WT sEH.

Phosphatase activity of sEH allelic variants toward LPAs

The catalytic activities of WT and six allelic variants of sEH toward LPAs, GGPP, and S1P were measured (Fig. II-3). The R103C and R287Q showed lower activities toward stearoyl-LPA and arachidonoyl-LPA than WT. The phosphatase activity of all allelic variants of sEH toward arachidoyl-LPA was very low and the suppression of the activity by the substitution of R103C or R287Q was not observed. These results suggest that arachidoyl-LPA (C20:0) is a poor substrate for sEH compared with arachidonoyl-LPA (C20:4) and stearoyl-LPA (C18:0).

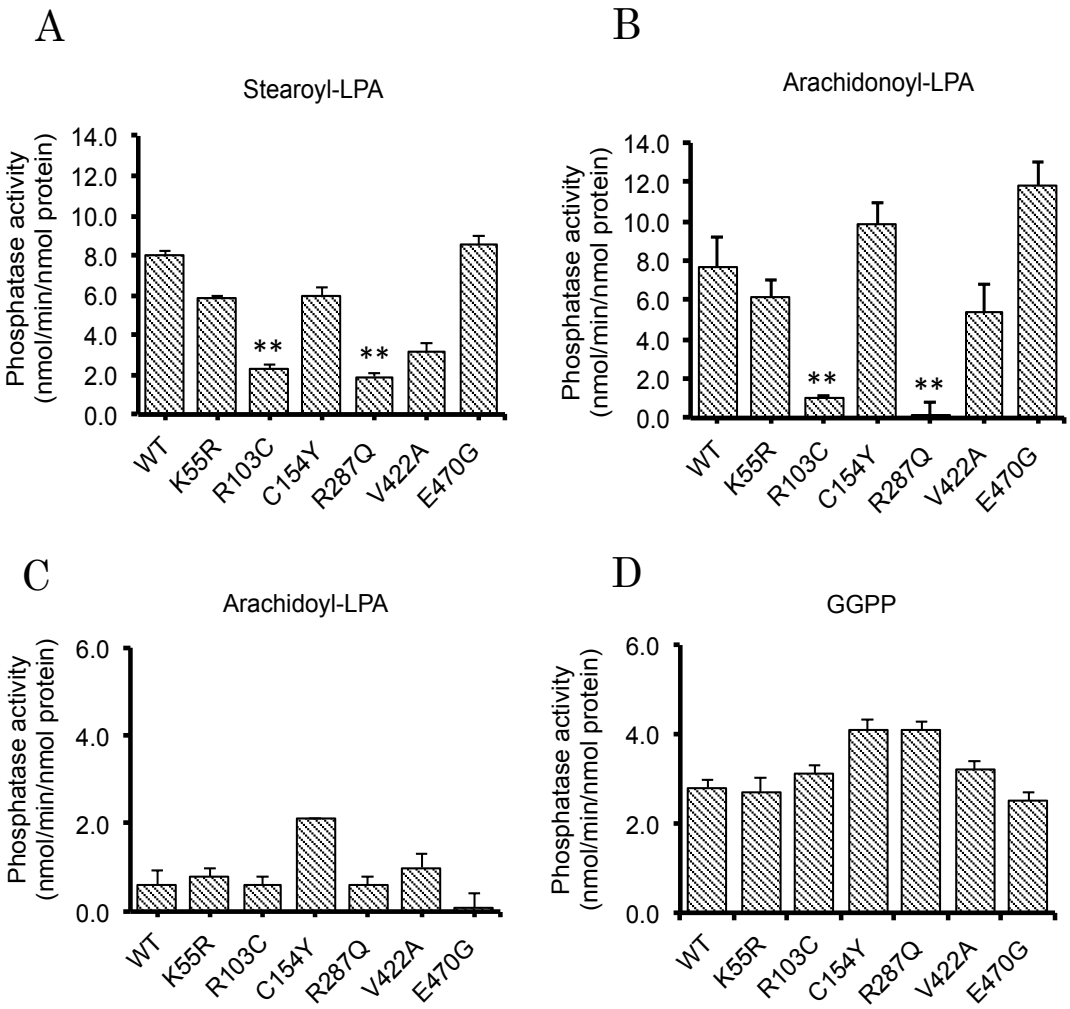

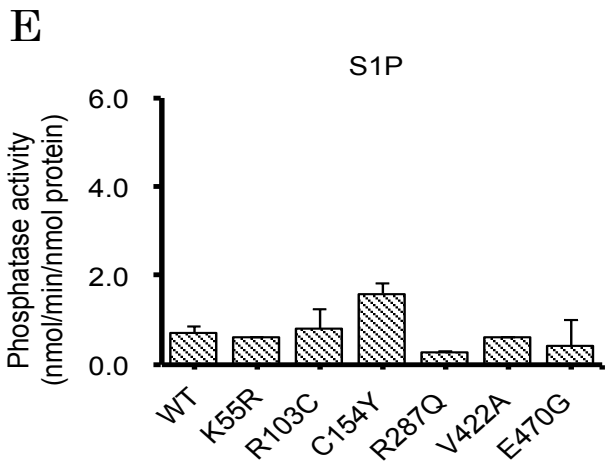

Fig. II-3 Phosphatase activities of full-length sEH allelic variants towards LPAs, GGPP, and S1P. Phosphatase activities of sEH allelic variants toward stearoyl-LPA (A), arachydonoyl-LPA (B), arachidoyl-LPA (C), GGPP (D), and S1P (E). Full-length WT and allelic variants (9.5 pmol) were incubated with each substrate (10 μM) at 37^0C for 5 min. The released phosphate was detected with malachite green. Values are given as the mean ± SD for three separate experiments. ** p<0.01, significantly different from WT sEH.

The activities of N-terminal allelic variants of sEH were also measured (Fig II-4). The activity of N-R103C toward stearoyl-LPA was significantly lower than that of the WT N-terminal domain. Otherwise, the N-R103C did not show significantly lower activities toward arachidonoyl-LPA, arachidoyl-LPA, GGPP, and S1P than the WT N-terminal domain. The N-K55R showed higher phosphatase activity toward LPAs, GGPP, and S1P than the WT.

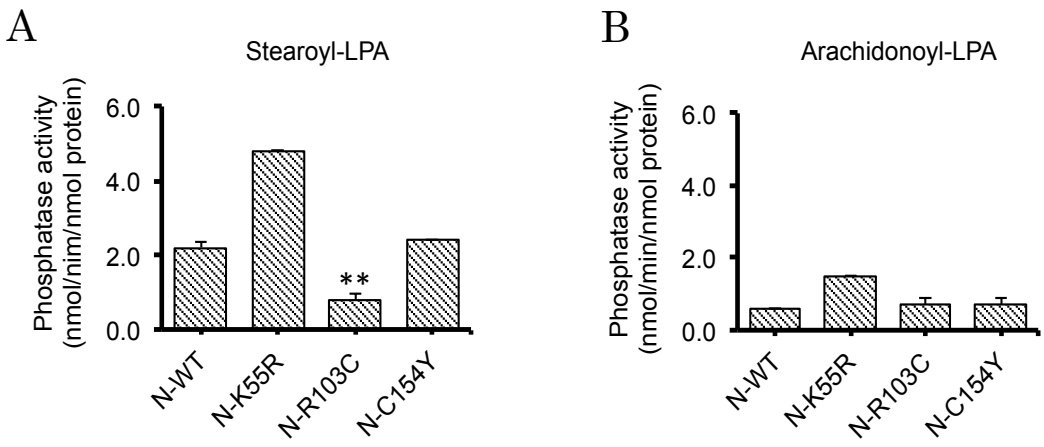

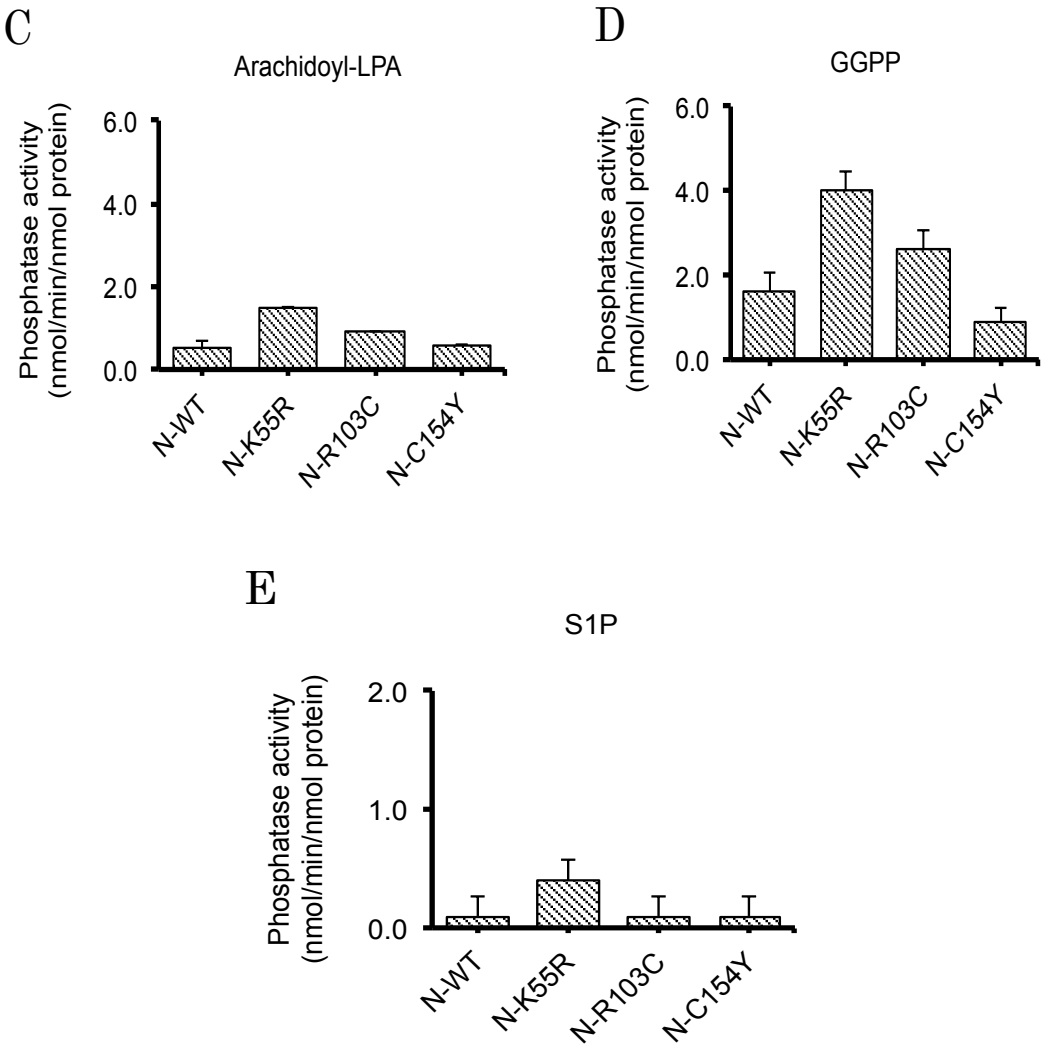

Fig. II-4 Phosphatase activities of the N-terminal allelic variants of sEH towards LPAs, GGPP, and S1P. The N-terminal allelic variant of sEH (9.5 pmol) was incubated with 10 μM stearoyl-LPA (A), arachydonoyl-LPA (B), arachidoyl-LPA (C), GGPP (D), and S1P (E). The released phosphate was detected with malachite green. Values are given as the mean ± SD for three separate experiments. $^{**}p<0.01$, significantly different from the WT sEH.

VEGF mRNA levels in Hep3B cells overexpressing sEH allelic variants

Previously our laboratory found that WT sEH suppressed *VEGF* mRNA levels in Hep3B cells, and the phosphatase domain of sEH was necessary for the suppression [19]. Therefore, I next examined the effect of amino acid

substitution on *VEGF* expression (Fig. II-5). The overexpression of the WT or sEH variants in Hep3B cells was confirmed by western blotting with anti-sEH antibody. The WT sEH suppressed *VEGF* mRNA levels compared with the levels in mock-treated cells, and five of the six sEH variants-i.e., all variants except V442A-showed a level of suppression similar to that of the WT sEH.

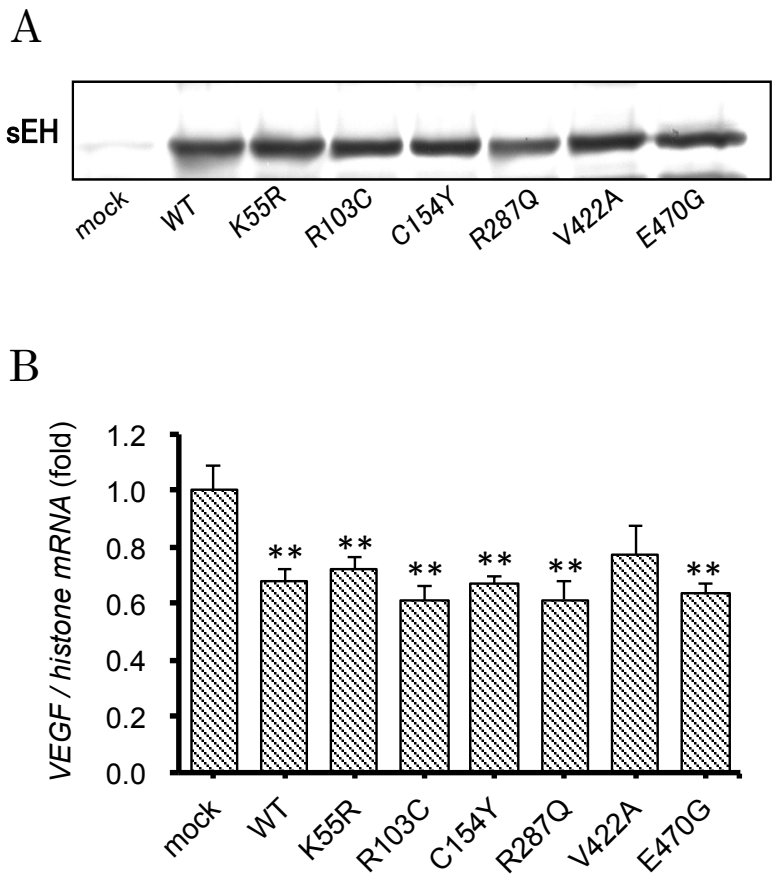

Fig. II-5 *VEGF* expression in the cells overexpressing the sEH allelic variants
(A) The overexpression of the WT or allelic variants of sEH in Hep3B cells was confirmed by western blotting with anti-sEH antibody. (B) *VEGF* mRNA levels were analyzed by real-time PCR. The ratio of *VEGF* to *histone-H4* mRNA in mock-treated cells was set at 1. VEGF: vascular endothelial growth factor. Values are the mean ± S.D. for three separate experiments. $^{**}p<0.01$, significantly different from mock treatment.

Kinetic determination of allelic variants toward LPA

Next, the kinetic parameters of sEH allelic variants toward stearoyl-LPA were determined (Table II-2). R103C and R287Q showed significantly lower *V*max values than the WT sEH, while *km* values of these variants were not significantly different from that of WT. R103C and R287Q also showed lower *V*max/*K*m ratios than the WT or other allelic variants of sEH (Fig. II-6).

TABLE II-2. Kinetic analysis of sEH allelic variants towards stearoyl-LPA

	*K*m (μM)	*V*max (nmol/min/nmol protein)	*V*max/*K*m
WT	12.1 ± 2.1	12.1 ± 1.0	1.00
K55R	8.9 ± 1.8	7.9 ± 0.7	0.89
R103C	7.2 ± 1.2	3.4 ± 0.2	0.47
C154Y	12.9 ± 2.7	11.6 ± 1.2	0.90
R287Q	8.9 ± 0.7	5.1 ± 0.3	0.57
V422A	9.1 ± 1.9	7.2 ± 0.7	0.79
E470G	16.7 ± 3.3	15.1 ± 1.6	0.90

The phosphatase activities of sEH allelic variants toward stearoyl-LPA were detected by malachite green, and the kinetic parameters of sEH allelic variants were analyzed. *K*m and *V*max values were calculated using Prism Graphpad enzyme kinetic software. Results are means ± SD (*n*=3).

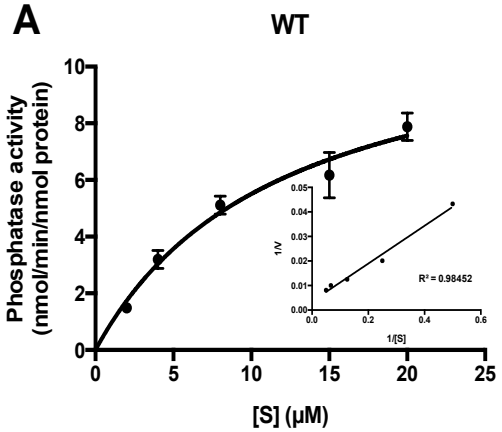

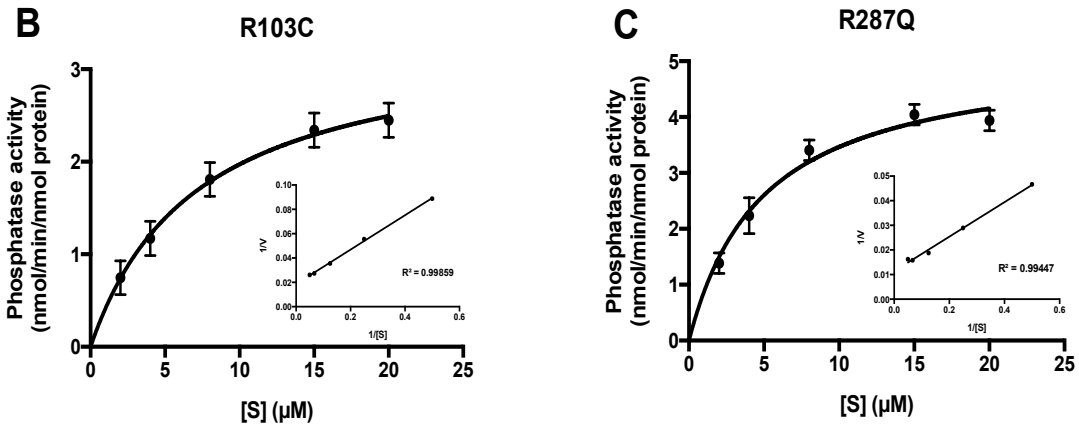

Fig. II-6. Determination of kinetic constants.
(A, B, C) sEH allelic variants (0.6 μg) were incubated with 0-20 μM of stearoyl-LPA, and incubated for 5 min at 37^0C in 25 mM Bis Tris-HCl buffer, pH 7.0, containing 1 mM $MgCl_2$ and 0.01% BSA. The kinetic constants were calculated by linear fitting of the Michaelis-Menten equation using enzyme Prism Graphpad kinetic software. Results are means ± SD (*n*=3).

II.4 Discussion

In a previous study, we found that LPAs were good substrates for the phosphatase activity of sEH [4]. In this study, I examined the metabolism of LPAs by allelic variants of human sEH. In the kinetic study, the R103C and R287Q had lower *V*max/*K*m ratios toward stearoyl-LPA than WT. In regard to the role of arginine residue, a crystal structure of mouse sEH showed that Arg^{285} (287 in human) forms an inter-monomer ionic salt bridge with Glu^{252}, and such salt-bridges are known to play an important role in protein structure and stabilization [10]. R103C and R287Q have been implicated in susceptibility to cardiovascular disease and stroke outcomes [13,14]. The allelic frequency of these variants was observed for diseases-susceptibility in African-American and Asian individuals including Japanese population. The greater allelic frequency of R103C and R287Q is approximately 17% in African-American and 21% in Asian individuals, respectively [9,60,61]. In this study, phosphatase activity of sEH toward arachidoyl-LPA was lower than those toward stearoyl-LPA and arachidonoyl-LPA. Despite the difference of only two-carbon length of acyl chain between arachidoyl- and stearoyl-LPA, arachidoyl-LPA which has longer acyl chain might not be able to fit the active pocket of sEH. On the other hand, compact molecular structure of arachidonoyl-LPA which has unsaturated acyl chain might result in fit to the active pocket of sEH. Due to the lower basal activity of full-length sEH toward arachidoyl-LPA, R103C and R287Q might not suppress the activity. sEH showed higher phosphatase activity toward LPAs than GGPP and S1P, suggesting that lyso-glycerophospholipids are specific substrates for the phosphatase activity of sEH.

The catalytic activities of sEH reported so far can be explained by the action of the N/C-terminal domain alone [62]. In this study, the full-length and the N-terminal domain alone of sEH displayed phosphatase activity toward

LPAs. The full-length and the C-terminal domain alone of sEH displayed epoxide hydrolase activity toward PHOME. These findings suggest that the presence of a phosphatase domain did not affect the epoxide hydrolase activity and the presence of epoxides hydrolase domain did not affect the phosphatase activity, indicating that both catalytic domain act independently.

In the current investigation, I found that the epoxide hydrolase activity of sEH toward PHOME was more sensitive to the amino acid substitution of allelic variants than that toward *t*-SO. I consider that epoxide hydrolase activity toward *t*-SO was hardly affected by the changes in the structure of active pocket by amino acid substitution, because molecular size of *t*-SO was smaller than that of PHOME. The R103C and R287Q had significantly lower epoxide hydrolase activity toward PHOME than WT sEH. The substitution of K55R and C154Y also slightly decreased epoxide hydrolase activity although these substitutions were present in N-terminal domain. Reduced epoxide hydrolase activity of mouse R103C sEH due to its unstable structure by the disruption of salt bridge with W142 has been suggested by Przybyla-Zawislak[9]. In the independent N/C-domains, some variants had similar activity when compared with the full-length of sEH, suggesting that these domains are independent of each other.

In conclusion, I found that the *in vitro* enzymatic activity of R103C or R287Q of sEH allelic variants was significantly different from WT on LPA hydrolysis and this may contribute to some of the pathologies associated with such polymorphisms studies. Previously it was found that overexpression of sEH suppressed VEGF expression in Hep3B cells, and the phosphatase activity was important in the suppression [19]. However, the *in vivo* investigations revealed that all allelic variants of sEH used in this experiment, except V442A, showed VEGF-suppressive effects similar to those of the WT sEH. These results suggest that the phosphatase activities of the sEH variants were sufficient to suppress the VEGF levels, even though these activities were lower than that of

the WT. Further investigation of the allelic variants identified herein could help to clarify the roles of the phosphatase activity of sEH.

General conclusion

In Chapter I, I characterized the frog homolog (*Xenopus laevis*) of human sEH and suggested the possible role of *Xenopus* sEH in the embryonic developmental. *In situ* hybridization and immunohistochemistry showed the sEH gene expression patterns during embryonic development, and in various tissues the expression was investigated both at the transcript and protein levels. In addition, the endogenous EETs, a substrate of sEH was detected in *Xenopus* liver. The human chimeras and mutants could explain the frog sEH has some different function with the human sEH. I also proved that frog sEH still be found to regulate epoxy fatty acid *in vivo* by *in vitro* determination of sEH endogenous substrates of 11,12-EET and 14,15-EET in frog tissues using LC-MS assay. EETs and sEH epoxide hydrolase activity seem to be important for development of *Xenopus*, but the phosphatase activity does not because the *Xenopus* sEH did not have phosphatase activity. This work is important knowledge and useful tool for further investigations on the development study of *Xenopus* sEH.

In Chapter II, the LPAs metabolism and VEGF expression by allelic variants of human sEH were examined by expressing in Hep3B cells. As a result, five of six allelic variants suppressed *VEGF* mRNA levels in Hep3B cells, and R103C or R287Q variant showed lower phosphatase activity toward LPAs. The data of VEGF-suppressive effect and the LPAs metabolism by the sEH allelic variants are the important finding in this study. These results may contribute to understanding the enzyme function for human diseases to develop drugs, and the possible role in future investigation of developmental study.

References

1) Morisseau C, Hammock BD. Epoxide hydrolases: mechanisms, inhibitor designs, and biological roles. *Annu. Rev. Pharmacol. Toxicol.,* **45**: 311-333 (2005).

2) Thomson SJ, Askari A, Bishop-Bailey D. Anti-inflammatory effects of epoxyeicosatrienoic acids. *Int. J. Vasc. Med.,* **2012**: 605101 (2012).

3) Fromel T, Jungblut B, Hu J, Trouvain C, Barbosa-Sicard E, Popp R, Liebner S, Dimmeler S, Hammock BD, Fleming I. Soluble epoxide hydrolase regulates hematopoietic progenitor cell function via generation of fatty acid diols. *Proc. Natl. Acad. Sci. U S A,* **109**: 9995-10000 (2012).

4) Oguro A, Imaoka S. Lysophosphatidic acids are new substrates for the phosphatase domain of soluble epoxide hydrolase. *J. Lipid Res.,* **53**: 505-512 (2012).

5) Enayetallah AE, Grant DF. Effects of human soluble epoxide hydrolase polymorphisms on isoprenoid phosphate hydrolysis. *Biochem. Biophys. Res. Commun.,* **341**: 254-260 (2006).

6) Cronin A, Mowbray S, Durk H, Homburg S, Fleming I, Fisslthaler B, Oesch F, Arand M. The N-terminal domain of mammalian soluble epoxide hydrolase is a phosphatase. *Proc. Natl. Acad. Sci. U S A,* **100**: 1552-1557 (2003).

7) Harris TR, Morisseau C, Walzem RL, Ma SJ, Hammock BD. The cloning and characterization of a soluble epoxide hydrolase in chicken. *Poult. Sci.,* **85**: 278-287 (2006).

8) Harris TR, Aronov PA, Hammock BD. Soluble epoxide hydrolase homologs in Strongylocentrotus purpuratus suggest a gene duplication event and subsequent divergence. *DNA and Cell Biology,* **27**: 467-477 (2008).

9) Przybyla-Zawislak BD, Srivastava PK, Vazquez-Matias J, Mohrenweiser HW, Maxwell JE, Hammock BD, Bradbury JA, Enayetallah AE, Zeldin DC, Grant DF. Polymorphisms in human soluble epoxide hydrolase. *Mol. Pharmacol.,* **64**: 482-490 (2003).

10) Srivastava PK, Sharma VK, Kalonia DS, Grant DF. Polymorphisms in human soluble epoxide hydrolase: effects on enzyme activity, enzyme stability, and quaternary structure. *Arch. Biochem. Biophys.,* **427**: 164-169 (2004).

11) Sinal CJ, Miyata M, Tohkin M, Nagata K, Bend JR, Gonzalez FJ. Targeted disruption of soluble epoxide hydrolase reveals a role in blood pressure regulation. *J. Biol. Chem.,* **275**: 40504-40510 (2000).

12) Schmelzer KR, Kubala L, Newman JW, Kim IH, Eiserich JP, Hammock BD. Soluble epoxide hydrolase is a therapeutic target for acute inflammation. *Proc. Natl. Acad. Sci. U S A,* **102**: 9772-9777 (2005).

13) Koerner IP, Jacks R, DeBarber AE, Koop D, Mao P, Grant DF, Alkayed NJ. Polymorphisms in the human soluble epoxide hydrolase gene EPHX2 linked to neuronal survival after ischemic injury. *J. Neurosci.,* **27**: 4642-4649 (2007).

14) Sato K, Emi M, Ezura Y, Fujita Y, Takada D, Ishigami T, Umemura S, Xin Y, Wu LL, Larrinaga-Shum S, Stephenson SH, Hunt SC, Hopkins PN. Soluble epoxide hydrolase variant (Glu287Arg) modifies plasma total cholesterol and triglyceride phenotype in familial hypercholesterolemia: intrafamilial association study in an eight-generation hyperlipidemic kindred. *J. Hum. Genet.,* **49**: 29-34 (2004).

15) Fornage M, Boerwinkle E, Doris PA, Jacobs D, Liu K, Wong ND. Polymorphism of the soluble epoxide hydrolase is associated with coronary artery calcification in African-American subjects - The Coronary Artery Risk Development in Young Adults (CARDIA) study. *Circulation,* **109**: 335-339 (2004).

16) Ohtoshi K, Kaneto H, Node K, Nakamura Y, Shiraiwa T, Matsuhisa M, Yamasaki Y. Association of soluble epoxide hydrolase gene polymorphism with insulin resistance in type 2 diabetic patients. *Biochem. Biophys. Res. Commun.,* **331**: 347-350 (2005).

17) Tokumura A, Fukuzawa K, Tsukatani H. Effects of synthetic and natural lysophosphatidic acids on the arterial blood pressure of different animal species. *Lipids,* **13**: 572-574 (1978).

18) Xu Y, Fang XJ, Casey G, Mills GB. Lysophospholipids activate ovarian and breast cancer cells. *J. Biochem.,* **309**: 933-940 (1995).

19) Oguro A, Sakamoto K, Suzuki S, Imaoka S. Contribution of hydrolase and phosphatase domains in soluble epoxide hydrolase to vascular endothelial growth factor expression and cell growth. *Biol. Pharm. Bull.,* **32**: 1962-1967 (2009).

20) Grant DF, Storms DH, Hammock BD. Molecular cloning and expression of murine liver soluble epoxide hydrolase. *J. Biochem,* **268**: 17628-17633 (1993).

21) Newman JW, Morisseau C, Harris TR, Hammock BD. The soluble epoxide hydrolase encoded by EPXH2 is a bifunctional enzyme with novel lipid phosphate phosphatase activity. *Proc. Natl. Acad. Sci. U S A,* **100**: 1558-1563 (2003).

22) Gomez GA, Morisseau C, Hammock BD, Christianson DW. Structure of human epoxide hydrolase reveals mechanistic inferences on bifunctional catalysis in epoxide and phosphate ester hydrolysis. *J. Biochem.,* **43**: 4716-4723 (2004).

23) Cronin A, Homburg S, Durk H, Richter I, Adamskal M, Frere F, Arand M. Insights into the Catalytic Mechanism of Human sEH Phosphatase by Site-Directed Mutagenesis and LC-MS/MS Analysis. *J. Mol. Biol.,* **383**: 627-640 (2008).

24) Yu Z, Davis BB, Morisseau C, Hammock BD, Olson JL, Kroetz DL, Weiss RH. Vascular localization of soluble epoxide hydrolase in the human kidney. *Am. J. Physiol. Renal Physiol.,* **286**: F720-726 (2004).

25) Arand M, Grant DF, Beetham JK, Friedberg T, Oesch F, Hammock BD. Sequence similarity of mammalian epoxide hydrolases to the bacterial haloalkane dehalogenase and other related proteins. Implication for the potential catalytic mechanism of enzymatic epoxide hydrolysis. *FEBS Lett.,* **338**: 251-256 (1994).

26) Spector AA, Norris AW. Action of epoxyeicosatrienoic acids on cellular function. *Am. J. Physiol-Cell Physiol,* **292**: C996-C1012 (2007).

27) Iliff JJ, Alkayed NJ. Soluble Epoxide Hydrolase Inhibition: Targeting Multiple Mechanisms of Ischemic Brain Injury with a Single Agent. *J. Future Neurol.,* **4**: 179-199 (2009).

28) Luria A, Morisseau C, Tsai HJ, Yang J, Inceoglu B, De Taeye B, Watkins SM, Wiest MM, German JB, Hammock BD. Alteration in plasma testosterone levels in male mice lacking soluble epoxide hydrolase. *Am J Physiol. Endocrinol. Metab.,* **297**: E375-383 (2009).

29) Nieuwkoop PD, Faber J. Normal table of Xenopus laevis (Daudin) : a systematical and chronological survey of the development from the fertilized egg until the end of metamorphosis. Garland Pub., New York (1994).

30) Monsoro-Burq AH. A rapid protocol for whole-mount in situ hybridization on Xenopus embryos. *CSH Protoc,* **2007**: pdb prot4809 (2007).

31) Melton DA, Krieg PA, Rebagliati MR, Maniatis T, Zinn K, Green MR. Efficient in vitro synthesis of biologically active RNA and RNA hybridization probes from plasmids containing a bacteriophage SP6 promoter. *Nucleic. Acids Res.,* **12**: 7035-7056 (1984).

32) Yue H, Jansen SA, Strauss KI, Borenstein MR, Barbe MF, Rossi LJ, Murphy E. A liquid chromatography/mass spectrometric method for simultaneous analysis of arachidonic acid and its endogenous eicosanoid metabolites prostaglandins, dihydroxyeicosatrienoic acids, hydroxyeicosatetraenoic acids, and epoxyeicosatrienoic acids in rat brain tissue. *J. Pharm. Biomed. Anal,* **43**: 1122-1134 (2007).

33) Zhang JH, Pearson T, Matharoo-Ball B, Ortori CA, Warren AY, Khan R, Barrett DA. Quantitative profiling of epoxyeicosatrienoic, hydroxyeicosatetraenoic, and dihydroxyeicosatetraenoic acids in human intrauterine tissues using liquid chromatography/electrospray ionization tandem mass spectrometry. *Anal. Biochem.,* **365**: 40-51 (2007).

34) Decker M, Arand M, Cronin A. Mammalian epoxide hydrolases in xenobiotic metabolism and signalling. *Arch. Toxicol.,* **83**: 297-318 (2009).

35) Morisseau C, Goodrow MH, Dowdy D, Zheng J, Greene JF, Sanborn JR, Hammock BD. Potent urea and carbamate inhibitors of soluble epoxide hydrolases. *Proc. Natl. Acad. Sci. U S A,* **96**: 8849-8854 (1999).

36) Lacourciere GM, Armstrong RN. Microsomal and soluble epoxide hydrolases are members of the same family of C-X bond hydrolase enzymes. *Chem. Res. Toxicol.,* **7**: 121-124 (1994).

37) Borhan B, Jones AD, Pinot F, Grant DF, Kurth MJ, Hammock BD. Mechanism of Soluble Epoxide Hydrolase - Formation of an Alpha-Hydroxy Ester-Enzyme Intermediate through Asp-333. *J. Biochem.,* **270**: 26923-26930 (1995).

38) Arand M, Wagner H, Oesch F. Asp333, Asp495, and His523 form the catalytic triad of rat soluble epoxide hydrolase. *J. Biochem.,* **271**: 4223-4229 (1996).

39) Argiriadi MA, Morisseau C, Hammock BD, Christianson DW. Detoxification of environmental mutagens and carcinogens: structure, mechanism, and evolution of liver epoxide hydrolase. *Proc. Natl. Acad. Sci. U S A,* **96**: 10637-10642 (1999).

40) Harris TR, Aronov PA, Jones PD, Tanaka H, Arand M, Hammock BD. Identification of two epoxide hydrolases in Caenorhabditis elegans that metabolize mammalian lipid signaling molecules. *Arch. Biochem. Biophysics.,* **472**: 139-149 (2008).

41) Yung YC, Stoddard NC, Chun J. LPA Receptor Signaling: Pharmacology, Physiology, and Pathophysiology. *J. Lipid Res.* (2014).

42) Morisseau C, Schebb NH, Dong H, Ulu A, Aronov PA, Hammock BD. Role of soluble epoxide hydrolase phosphatase activity in the metabolism of lysophosphatidic acids. *Biochem. Biophys. Res. Commun.,* **419**: 796-800 (2012).

43) Inoue M, Rashid MH, Fujita R, Contos JJ, Chun J, Ueda H. Initiation of neuropathic pain requires lysophosphatidic acid receptor signaling. *Nat Med,* **10**: 712-718 (2004).

44) Imamura F, Horai T, Mukai M, Shinkai K, Sawada M, Akedo H. Induction of in vitro tumor cell invasion of cellular monolayers by lysophosphatidic acid or phospholipase D. *Biochem. Biophys. Res. Commun.,* **193**: 497-503 (1993).

45) Watanabe N, Ikeda H, Nakamura K, Ohkawa R, Kume Y, Aoki J, Hama K, Okudaira S, Tanaka M, Tomiya T, Yanase M, Tejima K, Nishikawa T, Arai M, Arai H, Omata M, Fujiwara K, Yatomi Y. Both plasma lysophosphatidic acid and serum autotaxin levels are increased in chronic hepatitis C. *J. Clin. Gast.,* **41**: 616-623 (2007).

46) Ye XQ. Lysophospholipid signaling in the function and pathology of the reproductive system. *Hum. Reprod. Update,* **14**: 519-536 (2008).

47) Rancoule C, Dusaulcy R, Treguer K, Gres S, Attane C, Saulnier-Blache JS. Involvement of autotaxin/lysophosphatidic acid signaling in obesity and impaired glucose homeostasis. *Biochimie.,* **96C**: 140-143 (2014).

48) Zhang ZH, Liu ZG, Meier KE. Lysophosphatidic acid as a mediator for proinflammatory agonists in a human corneal epithelial cell line. *Am. J. Physiol-Cell Physiol,* **291**: C1089-C1098 (2006).

49) Billon-Denis E, Tanfin Z, Robin P. Role of lysophosphatidic acid in the regulation of uterine leiomyoma cell proliferation by phospholipase D and autotaxin. *J. Lipid. Res.,* **49**: 295-307 (2008).

50) Gill SS, Hammock BD. Distribution and properties of a mammalian soluble epoxide hydrase. *Biochem. Pharmacol.,* **29**: 389-395 (1980).

51) Enayetallah AE, French RA, Thibodeau MS, Grant DF. Distribution of soluble epoxide hydrolase and of cytochrome P450 2C8, 2C9, and 2J2 in human tissues. *J. Histochem. Cytochem.,* **52**: 447-454 (2004).

52) Campbell WB. New role for epoxyeicosatrienoic acids as anti-inflammatory mediators. *Trends. Pharmacol. Sci.,* **21**: 125-127 (2000).

53) Iliff JJ, Wang RK, Zeldin DC, Alkayed NJ. Epoxyeicosanoids as mediators of neurogenic vasodilation in cerebral vessels. *Am. J. Physiol-Heart and Cir. Physiol.,* **296**: H1352-H1363 (2009).

54) Shen GF, Jiang JG, Fu XN, Wang DW. [Promotive effects of epoxyeicosatrienoic acids (EETs) on proliferation of tumor cells]. *Ai Zheng,* **27**: 1130-1136 (2008).

55) Morisseau C, Wecksler AT, Deng C, Dong H, Yang J, Lee KS, Kodani SD, Hammock BD. Effect of Soluble Epoxide Hydrolase Polymorphism on Substrate and Inhibitor Selectivity, and Dimer Formation. *J. Lipid Res.* (2014).

56) Fava C, Montagnana M, Danese E, Almgren P, Hedblad B, Engstrom G, Berglund G, Minuz P, Melander O. Homozygosity for the EPHX2 K55R

polymorphism increases the long-term risk of ischemic stroke in men: a study in Swedes. *Pharmaco. Gen.,* **20**: 94-103 (2010).

57) EnayetAllah AE, Luria A, Luo B, Tsai HJ, Sura P, Hammock BD, Grant DF. Opposite regulation of cholesterol levels by the phosphatase and hydrolase domains of soluble epoxide hydrolase. *J. Biol. Chem.,* **283**: 36592-36598 (2008).

58) Sako A, Kitayama J, Shida D, Suzuki R, Sakai T, Ohta H, Nagawa H. Lysophosphatidic acid (LPA)-induced vascular endothelial growth factor (VEGF) by mesothelial cells and quantification of host-derived VEGF in malignant ascites. *J. Surg. Res.,* **130**: 94-101 (2006).

59) Xie Y, Liu Y, Gong G, Smith DH, Yan F, Rinderspacher A, Feng Y, Zhu Z, Li X, Deng SX, Branden L, Vidovic D, Chung C, Schurer S, Morisseau C, Hammock BD, Landry DW. Discovery of potent non-urea inhibitors of soluble epoxide hydrolase. *Bioorg. Med. Chem. Lett.,* **19**: 2354-2359 (2009).

60) Saito S, Iida A, Sekine A, Eguchi C, Miura Y, Nakamura Y. Seventy genetic variations in human microsomal and soluble epoxide hydrolase genes (EPHX1 and EPHX2) in the Japanese population. *J. Hum. Genet.,* **46**: 325-329 (2001).

61) Sandberg M, Hassett C, Adman ET, Meijer J, Omiecinski CJ. Identification and functional characterization of human soluble epoxide hydrolase genetic polymorphisms. *J. Biol. Chem.,* **275**: 28873-28881 (2000).

62) Purba ER, Oguro A, Imaoka S. Isolation and characterization of Xenopus soluble epoxide hydrolase. *Biochim. Biophys. Acta.* **7**:954-62 (2014).

Abbreviations

sEH, soluble epoxide hydrolase
CYP P450, cytochrome P450
EET, epoxyeicosatreienoic acid
DHET, dihydroxyeicosatrienoic acid
WISH, whole-mount in situ hybridization
sLPA, stearoyl L-α-lysophosphatidic acid
arachidonoyl LPA, arachidonoyl L-α-lysophosphatidic acid arachidoyl LPA, arachidoyl L-α-lysophosphatidic acid
GGPP, geranylgeranyl pyrophosphate
S1P, sphingosine-1-phosphate
RT-PCR, reverse-transcription polymerase chain reaction
VEGF, vascular endothelial growth factor
4-MUP, 4-methylumbelliferyl phosphate
PHOME, 3-phenyl-cyano methyl ester-2-oxiraneacetic acid
t-SO, *trans* stilbene oxide.

Bibliography

Publications:

1. Endang R. Purba, Ami Oguro and Susumu Imaoka, "Isolation and characterization of *Xenopus* soluble epoxide hydrolase", *Biochimia et Biophysica Acta*. *Mol. cell Biol. lipid.* 1841(7): 954-962, 2014
2. Endang R. Purba, Ami Oguro and Susumu Imaoka, "The metabolism of lysophosphatidic acids by allelic variants of human soluble epoxide hydrolase", *Drug Metab. Pharmacokinet.* 2014 (in press)

International congresses:

1. Endang R Purba, Ami Oguro and Susumu Imaoka, "The metabolism of lysophosphatidic acid by genetic variants of human soluble epoxide hydrolase", The 17th International Congress of Personal Medicine, Kobe -Japan, November 4, 2013.
2. Endang R Purba, Ami Oguro and Susumu Imaoka, "Difference of epoxide hydrolase and phosphatase activities in the six polymorphic variants of human soluble epoxide hydrolase", The XIII International Congress of Toxicology (ICT) COEX, Seoul - Korea, July 2, 2013.
3. Endang R Purba, Ami Oguro and Susumu Imaoka, "Identification and Comparison of EPHX2 (sEH) and EPHX4 (EH4) in *Xenopus laevis*", The 84th Annual Meeting of Japanese Biochemical Society, Fukouka - Japan, December 15, 2011.
4. Endang R Purba, Ami Oguro and Susumu Imaoka, "Characterization of *Xenopus* Soluble Epoxide Hydrolase during Embryonic Developmental", The 83th Annual Meeting of Japanese Biochemical Society, Kyoto - Japan, September 24, 2011.

Acknowledgement

I would like to express my thanks to Prof. Susumu Imaoka, School of Science, Department of Bioscience and Technology for encouragement, support, and motivation through this study.

Beside my advisor, I would like to thank the rest of my thesis committee: Prof. Kiyoshi Othani and Prof. Yoshiyuki Seki for their encouragement, insightful comments, and motivation.

My sincere thank also to Dr. Ami Oguro and my fellow lab-mates in Imaoka Laboratory for their kind and help.

This work was supported by the MEXT foundation, the Ministry of Education, Culture, Sports, Science and Technology, Japan.

Endang Rinawati Purba